TAMPEREEN TEKNILLINEN YLIOPISTO
TAMPERE UNIVERSITY OF TECHNOLOGY

Timo Salpavaara

Inductively Coupled Passive Resonance Sensors: Readout Methods and Applications

Julkaisu 1524 • Publication 1524

Tampere 2018

Tampereen teknillinen yliopisto. Julkaisu 1524
Tampere University of Technology. Publication 1524

Timo Salpavaara

Inductively Coupled Passive Resonance Sensors:
Readout Methods and Applications

Thesis for the degree of Doctor of Science in Technology to be presented with due permission for public examination and criticism in Sähkötalo Building, Auditorium SJ204, at Tampere University of Technology, on the 1st of March 2018, at 12 noon.

Tampereen teknillinen yliopisto - Tampere University of Technology
Tampere 2018

Doctoral candidate:	Timo Salpavaara Faculty of Biomedical Sciences and Engineering Tampere University of Technology Finland
Supervisor:	Professor Jukka Lekkala Faculty of Biomedical Sciences and Engineering Tampere University of Technology Finland
Pre-examiners:	Professor Robert Puers University of Leuven Belgium
	Professor Tapio Seppänen University of Oulu Finland
Opponent:	Professor Jerker Delsing Luleå University of Technology Sweden

ISBN 978-952-15-4079-0 (printed)
ISBN 978-952-15-4096-7 (PDF)
ISSN 1459-2045

Abstract

Measurement systems are used to acquire information from the surrounding world. The requirements of the measurement system depend on the application, and the acquired information is used in different ways. For example, measurements are taken as part of the control systems of industrial processes. Alternatively, the information obtained from the measurements can be used to provide answers to scientific questions. Each measurement has a case-specific importance for the user and a certain cost in terms of time and money. Therefore, the same measurement approach is not optimal in every case. The design process of the measurement systems always includes a compromise between performance, viability, and cost. These factors are, in turn, strongly dependent on the implementation of the measurement system in each separate case. Inductively coupled passive resonance sensors provide a measurement method that has two notable benefits: the simple structure of the sensors and the possibility to take short-range wireless measurements. However, the limitations of the available readout devices have often impeded the use and development of these sensors in many demanding applications. In addition, uncertainty in the measurement results due to inductive coupling hinders the use of this method.

This work concerns the development and implementation of a measurement system based on inductively coupled passive resonance sensors. A custom-made readout device to improve the feasibility of the readout in applications where continuous field measurements are performed was both specified and produced. The readout device was implemented using a simplified version of the method used in conventional impedance analyzers. In addition, signal processing methods were developed which can extract resonance characteristics from the measured data. A special algorithm was developed to compensate for the effects of the changes in the inductive coupling when the measurement distance varies. The operation of the developed readout methods was studied using simulations, and several realistic measurement configurations were tested. Competing readout methods published in the literature were also simulated. The accuracy of all the studied methods depended on the configuration of the measurement system. The inductive coupling coefficient also had a significant influence on the accuracy of the tested methods.

The newly-developed readout methods and the inductively coupled passive resonance sensor were then utilized in a medical application to monitor the pressure between the skin and compression garments. These garments are used, for example, to improve the healing of burns and reduce swelling in the legs. Effective medical treatment of such conditions requires that the appropriate pressure is applied. With this system, the pressure reading under the compression garment can be obtained by using simple disposable sensors that can be read wirelessly through a thin fabric. Using our inductive coupling compensation method, the sensor enabled the monitoring of the pressure with the required level of precision.

Inductively coupled resonance sensors can also be used to monitor the properties of the materials around the sensor. This monitoring is possible because the permittivity of the environment near to the sensor affects the sensor's resonance characteristics. This method was tested in two applications. In the first application, the manufacturing process of ceramic slurry was monitored by a sensor that was installed inside the container where the slurry was mixed. The resonance characteristics of the sensor were measured as the manufacturing process was incrementally carried out. The results indicated that the method could be used to control the composition of the slurry. In the second application, the inductively coupled sensors were tested in monitoring the degradation processes of two different polymers during hydrolysis. In this application, the sensors were encapsulated into the tested polymers. The polymer samples were kept inside containers filled with buffer solution and the resonance characteristics of the encapsulated sensors were then measured wirelessly from outside. The results showed a clear difference in degradation profiles between the tested polymers. The method may provide a novel way to continuously monitor the degradation processes of certain materials.

In summary, the developed readout methods improved the applicability of inductive coupled passive resonance sensors in the tested applications and created novel ways to acquire information. This new technology provides a good starting point for the development of a new generation of inductively coupled passive resonance sensors.

Preface

I would like to express my gratitude to my supervisor professor Jukka Lekkala for his guidance and support throughout this study. I am also grateful for my position in his research group. I highly appreciate the work done by the pre-examiners. Professor Tapio Seppänen and Professor Robert Puers have done excellent and huge work in reviewing the thesis and suggesting improvements. In addition, I want to acknowledge the efforts of professor Minna Kellomäki, professor Matti Vilkko, professor Erkki Levänen and Markku Honkala in organizing the projects where I was allowed carry out the research. I want to express my gratitude to Jarmo Verho and Pekka Kumpulainen for their contributions to the publications included in this thesis and their advice on research and technology in general. I am grateful to Ville Rantanen and Terho Jussila, both of whom gave me valuable advice about the thesis manuscript. In addition, I want thank all the other co-authors and all who have volunteered to comment on the thesis manuscript. I also want to thank Antti Vehkaoja, Jouko Halttunen and Heimo Ihalainen for their advice. In addition, I am grateful to everyone in the former Department of Automation Science and Engineering for discussions and friendly atmosphere in the department.

The research for this thesis was performed at Tampere University of Technology (TUT) and more specifically at the Department of Automation Science and Engineering and at the Faculty of Biomedical Sciences and Engineering (2017–). The work has been carried out during projects that were funded by the Finnish Funding Agency for Technology and Innovation (Tekes) and several private companies, for whose financial support I am grateful. I also want to thank the Finnish Foundation of Automation for the travel grants that allowed me to attend several conferences. This encouraged me to publish many of the articles that are discussed in this thesis.

Tampere 19.12.2017

Timo Salpavaara

Contents

Abbreviations

AD8302	RF/IF gain and phase detector by Analog Devices
ADC	analog-to-digital converter
AM	amplitude modulation
DDS	direct digital synthesis
ANFIS	adaptive-network-based fuzzy inference system
ECG	electrocardiography
HF	high frequency
HP	high-pass
IF	intermediate frequency
I-V method	a method used in some impedance analyzers to determine impedance
LC	electrical circuit consisting of coil and capacitor
LP	low-pass
PCA	principal component analysis
PCL	polycaprolactone
PE	polyethylene
PET	polyethylene terephthalate
pH	numeric scale used to specify acidity or basicity
PLA	polylactic acid
PDMS	polydimethylsiloxane
PCB	printed circuit board
RFID	radio-frequency identification
RLC	electrical circuit consisting of resistor, coil and capacitor
SMA	connector type (SubMiniature version A)
Q	quality factor
UHF	ultra high frequency
USB	universal serial bus
VHF	very high frequency
ZnO	zinc oxide

Symbols

BW_p	estimate of the width of the measured phase curve
BWG	estimate of the width of the measured gain curve
C_r	parallel capacitance of the reader coil
C_s	capacitance of the sensor
f	frequency
f_0	resonance frequency of the sensor
f_c	compensated resonance frequency estimate
f_{Lr}	self-resonance frequency of the reader coil
f_{max}	estimate for the frequency of the maximum in the real part of impedance
f_{md}	estimate for the frequency of the minimum in the measured phase curve
f_{mu}	estimate for the frequency of the maximum in the measured phase curve
f_p	estimate for the frequency of the minimum in the phase of impedance
FG	estimate for the frequency of the minimum in the measured gain curve
k	inductive coupling coefficient
L_1	inductance of the primary coil
L_2	inductance of the secondary coil
L_s	inductance of the sensor
M	mutual inductance
N_1	number of turns in primary coil
N_2	number of turns in secondary coil
p_1	first order coefficient of linear model
p_2	constant term of linear model
r_1	radius of the primary coil
r_2	radius of the secondary coil
R_r	resistance of the reader coil
R_s	resistance of the sensor
R_t	resistance of the component that is used to feed current to reader coil
S_{11}	input port voltage reflection coefficient (a scattering parameter)
V_t	ideal voltage source
V_m	ideal voltage measurement
x	distance between coils
X	equivalent impedance
Z_s	series impedance of the resonance sensor circuit
λ	wavelength
μ	permeability
ω	angular frequency
ω_0	angular frequency at f_0
Θ_d	value of the local minimum in the measured phase curve
Θ_u	value of the local maximum in the measured phase curve
Θ_m	estimate for the height of the measured phase curve

List of Publications

This thesis is based on five publications and one unpublished manuscript. The publications are referred in this thesis as [P1-P5] and the unpublished manuscript is referred as [M1].

PUBLICATIONS

P1. Salpavaara T., Verho J., Kumpulainen P. and Lekkala J., "Readout methods for an inductively coupled resonance sensor used in pressure garment application," *Sensors and Actuators A: Physical*, vol. 172, issue 1, pp. 109–116, Dec. 2011.

P2. Salpavaara T., Verho J. and Kumpulainen P., "Performance of a Near-Field Radio-Frequency Pressure Sensing Method in Compression Garment Application," In *Proceedings of Wireless Mobile Communication and Healthcare, MobiHealth 2011, Lecture Notes of the Institute for Computer Sciences, Social Informatics and Telecommunications Engineering*, vol. 83, pp. 322–328, 2012.

P3. Salpavaara T. and Lekkala J. "A model based analysis of the measurement errors in inductively coupled passive resonance sensors," In *Proceedings of XXI IMEKO World Congress*, Prague, Czech Republic, Aug. 30 - Sep. 4, 2015. 4 pages.

P4. Salpavaara T., Järveläinen M., Seppälä S., Yli-Hallila T., Verho J., Vilkko M., Lekkala J. and Levänen E., "Passive resonance sensor based method for monitoring particle suspensions," *Sensors and Actuators B: Chemical*, vol. 219, pp. 324–330, Nov. 2015.

P5. Salpavaara T., Antniemi A, Hänninen A., Lekkala J. and Kellomäki M. "Inductively coupled passive resonance sensor for monitoring biodegradable polymers in vitro," *Procedia Engineering*, vol. 168, pp. 1304-1307, Sep. 2016.

UNPUBLISHED MANUSCRIPT

M1. Salpavaara T, Verho J. and Lekkala J., "Simulation of Readout Methods for Inductively Coupled Passive Resonance Sensors"

The main contributions of the publications and the manuscript are:

P1. This journal paper describes the methods that are needed to perform wireless pressure measurements underneath compression garments using inductively coupled passive resonance sensors. The measurement system consists of a readout device, feature extraction methods, an inductive coupling compensation method and a pressure sensor.

P2. This publication includes further testing and feasibility studies of the methods introduced in [P1]. The publication describes the testing of a new sensor prototype and an investigation of the effects of the positioning and measurement environment on the acquired readings.

P3. The third publication illustrates a lumped element model and the simulations that were used to study the effects of the inductive coupling on the readout methods, which are based on impedance measurements.

P4. The fourth publication describes a measurement system that was designed for suspension monitoring. The method includes an embedded sensor set-up, readout device and signal processing. The method was tested by monitoring the fabrication of a suspension made of water, a dispersing agent and aluminium oxide.

P5. In the fifth article, the passive resonance sensors were applied to monitoring the degradation of polymers during hydrolysis. The measured signals were compared with the conventional material test measurements.

M1. The lumped element model and the simulations introduced in [P3] were used to compare the signal processing methods of the inductively coupled passive resonance sensors in situations where the reader coil configuration was varied. The paper also proposes that the lumped element model can be used to simulate the operation principle of the custom-made readout device. The possibility to compensate the changes in inductive coupling in the most common methods is also studied.

The author's role in the publications and the manuscript:

P1. The author planned, specified and tested the readout device with the second author but did not partake in the electrical or software design of the readout device. The author developed the feature extraction methods with the third author. The author is responsible for the design and testing of the inductive coupling compensation and the pressure sensor. The author wrote the main parts of the article.

P2. The author designed the sensors, planned and carried out the measurements and executed the signal processing excluding the ANFIS-model. The author wrote the main parts of the article.

P3. The author carried out the simulations and wrote the article.

P4. The author was responsible for the areas concerning the inductively coupled passive resonance measurements, excluding the custom-made readout device. He designed, planned and carried out the suspension measurements together with the second author. The author was responsible for the signal processing and analysed the results with the rest of the authors. The author was the main author of this publication and wrote the most of the article. The second author used the contributions related to material sciences in his doctoral thesis.

P5. The author planned the inductively coupled measurement set-up and executed the signal processing for this publication. The sensor design was planned in co-operation with Jarmo Verho. The encapsulation process of the sensors and the measurements were completed by the second author. The author was the main author of this publication and wrote the main parts of the article.

M1. The author carried out the simulations, signal processing and wrote the main parts of the manuscript.

1 Introduction

This thesis is about developing new technology for inductively coupled passive resonance sensors in order to make them a more viable option for demanding measurement applications.

1.1 Motivation

Measurements are needed to optimize and control the actions and processes in a variety of applications, ranging from industry to healthcare. In healthcare, the effectiveness and safety of a treatment may depend on the quality of the monitoring used to control the treatment. In practice, processes are not always monitored or controlled because there is no feasible or cost-effective measurement system available. Therefore, optimization of a measurement system and good feedback can not only improve the quality of any process, resulting in increased profits for industry, but it may also save lives.

Wireless sensors have provided solutions for many applications where conventional sensors are impractical. Wireless sensors can be used for healthcare [1], activity monitoring [2], structural health monitoring [3] and agriculture [4], [5]. The concept of using wireless sensors as a part of more complex entity, such as a network or an intelligent environment has also been frequently proposed [6]–[9].

The conventional implementation for a wireless sensor node is a complex electronic system that is realized by mounting the needed integrated circuits on a printed circuit board. The information is transmitted by electromagnetic waves. However, such complex systems are often delicate and expensive. The power management is a common problem which limits taking continuous or frequent measurements, because any portable power source eventually runs out of juice.

There are passive wireless measurement systems, such as modified RFID tags [10], which do not require an active electric power source like a battery. These systems take the power they need from the electromagnetic waves that are transmitted by the readout devices. However, this power transmission method is inefficient and limited by regulation. Thus, the available electric power still limits the generation of excitation signals, signal conditioning, and analog-to-digital conversion. In addition, wireless sensors based on transmitting and receiving electromagnetic waves have long communication ranges, and thus the data has to be encrypted.

As an alternative method, inductively coupled passive resonance sensors provide a means to make short-range wireless measurements using a very simple sensor. The measurement distance of inductive sensors is typically of the same order of magnitude as the dimension of the reader and the sensor coils. For example, in medical applications the distance is typically a few centimeters. These sensors are a valid option in applications where the measurement target is underneath a non-metallic surface, such as skin, fabric or a plastic casing, in addition to which, the short reading range is a benefit in respect of information security.

Inductively coupled passive sensors were successfully tested and reported in detail by Collins [11] in the sixties, and the method had been mentioned even earlier [12]. Nevertheless, in spite of its benefits, the method has never become very popular. The reason for this is that during their early development, (mid-20thC) the limitations of the readout electronics made the method cumbersome to use. However, nowadays complex readout electronics can be integrated into a conveniently small space. In addition, the simple structure of the actual sensor has encouraged the testing of unconventional fabrication methods and materials which can be used in their construction. Thus, inductively coupled passive resonance sensors have been fairly recently tested in many new applications [13].

There are various methods for acquiring and processing the data that inductively coupled passive resonance sensors provide. These methods are largely dependent on the application, the sensor, and the measurement set-up, and none of them have succeeded in making inductive coupled passive sensors popular over a wide range of applications. This leaves room for further development.

Another issue with these sensors is that the measuring chain of this method is more complicated than it is with more conventional measurement methods. One of the aims of this work is to identify the problematic or critical parts of this process and to develop technology which will improve the performance of the measurement system in the selected applications.

1.2 Scope

The measurement methods based on the inductively coupled passive resonance sensors were studied. In particular, the focus was on the readout methods based on frequency-response measurements. Instead of commercial impedance analyzers, a custom-made readout device was used. This made it more feasible to take the measurements and to allow testing of the equipment in challenging environments. This decision also influenced the signal-processing methods which were studied. In

this thesis, readout methods and signal processing were developed and tested in the selected applications. Each application required dedicated sensors. For example, the pressure under compression garments was measured using sensors with variable capacitive elements. On the other hand, the process substances were monitored by sensors whose parameters are modified by the permittivity of the immediate environment. A more detailed analysis of the sensors' properties is beyond the scope of this work.

1.3 Research questions and objectives

This thesis focuses on the measuring chain of inductively coupled passive resonance sensors. The purpose of the thesis is to identify the factors that limit the use of this measurement method, and to find solutions to those problems. The main research questions of this thesis are defined as follows:

1. What kind of readout methods are needed to increase the feasibility and versatility of inductively coupled passive resonance sensors?
2. How do the properties of the reader coil and the variations in inductive coupling affect the measured resonance curves and the extracted features?
3. Can the effects of an unknown inductive coupling on the estimates for the resonance frequency be compensated for?

The general goal of this thesis is to develop methods which promote the development and use of inductively coupled passive resonance sensors. The objectives for this thesis are as follows:

1. To find out the benefits and constraints of the measurement method.
2. To promote the testing of inductively coupled sensors in challenging applications by developing novel readout and signal processing methods.
3. To test the developed readout methods' ability to measure the pressure under compression garments.
4. To develop a measurement arrangement and signal processing for monitoring a suspension during a ceramic slurry manufacturing process.
5. To develop methods for monitoring the degradation processes of biodegradable materials.

1.4 Contribution

The main scientific contributions of this thesis are summarized in the following points:

- A new portable readout device for inductively coupled passive resonance sensors was developed and tested.
- Signal processing methods were developed to extract resonance characteristics from the data measured with the custom-made reader device.
- A special algorithm that compensates for the effects of the changes in the inductive coupling on the resonance frequency estimate was developed and tested.
- The operation of the developed readout method and other competing readout methods were studied using simulations in various cases where the inductive coupling and the reader coil configuration was varied.
- The developed readout methods and the customized resonance sensors were implemented in three applications:
    - A novel method for measuring the pressure under compression garments was developed and tested.
    - A novel method for monitoring the fabrication of ceramic suspensions was developed and tested.
    - A novel method for monitoring biodegradable polymers during hydrolysis was developed and tested.

1.5 Organization

This thesis is structured as follows. Chapter 1 defines the motivation, the scope of the thesis, the research questions, the contributions and the organization of the thesis. Chapter 2 provides the background to inductively coupled passive resonance sensors and the general principles of the measurement method. The background of each element in the measuring chain is briefly discussed. The developed readout methods and the related signal processing are presented in Chapter 3. This chapter gives answers to the first and third research questions. These methods were developed to improve the applicability of inductively coupled passive resonance sensors. An inductive coupling compensation algorithm is also presented and tested in this chapter, and the chapter finishes with a discussion of the developed readout methods. Chapter 4 covers the modelling and simulations of the inductively coupled passive resonance sensors. This chapter also includes discussion about the results of the simulations. These simulations, in part, were used to find answers to the second and

third research questions. The developed methods were applied to pressure measurements and material monitoring. Chapter 5 gives an introduction to the tested applications, all of which provide a suitable context and purpose for the developed technology. This chapter also presents and discusses the results from the applications. Chapter 6 presents the author's conclusions and indicates areas for future research.

2 Background

2.1 Inductively coupled passive resonance sensors

Inductively coupled passive resonance sensors are based on a measurement concept where the measured quantity or measurand [14] alters the impedance of a resonance circuit consisting of a coil and a capacitor. The resonance circuit is wirelessly measured using an inductive coupling. The inductive coupling is formed between a reader coil and the coil in the resonator circuit. Because of this coupling, the measurand affects the measured impedance of the reader coil.

The information is transferred via a magnetic field. This is the main characteristic that distinguishes inductively coupled passive resonance sensors from the other wireless sensors that use electromagnetic waves or an electric field as a medium to transfer information. The reading ranges of inductively coupled sensors are much shorter than in the methods that use electromagnetic waves [15]. In this method, the readout device provides the excitation energy that is used in the measurement. Because of the inductive coupling, there is no need to have any active power sources like batteries in the sensor part. Thus, the sensors are called passive, as opposed to active sensors, which have their own power source.

Besides the inductive coupling, the other typical characteristic of this concept is that the inductively transmitted excitation energy is resonating in the sensor between the magnetic and electric fields. Thus, the sensor has a resonance frequency where the imaginary parts of the impedance of the coil and capacitor cancel each other out. The resonance sensors can be measured by determining the impedance of the reader coil at discrete frequencies near to the approximated resonance frequency. Around this resonance frequency, the sensor creates clearly detectable deviations (a resonance curve) into the measured impedance of the reader coil.

The measurand is tied to the impedance of the sensor and can be detected from the measurement of the reader coil. If the measured quantity affects either the coil, or the capacitance of the sensor, the frequency of the measured resonance curve is altered. On the other hand, the measurand can be made to affect the resistance of the sensor. In this case, the changes in the resistance modify the properties of the resonance curve.

2.2 Closely related methods

Wireless measurements are often based on sensor nodes, which consist of sensing elements, an analog front end, an analog-to-digital converter, a microprocessor, a power supply, power management, radio interface circuitry and an antenna. In short, these kinds of sensor nodes have a similar measuring chain to wired measurement systems, but the data is transmitted using electromagnetic waves. The wireless sensor nodes have long operating ranges. The active power sources allow the use of efficient signal conditioning, and the microprocessor in the sensor node enables relatively complicated data processing options. The data transfer rates, energy efficiency, operating frequency, and topology of wireless sensor networks depend on the used radio technology [16], [17]. The main drawbacks with this approach are the size and complexity of the sensor nodes and the fact that the power source eventually runs out of energy and needs to be recharged.

It is also possible to transmit data via a magnetic field, as has been shown in [18], for example. These sensors use two coils instead of antennae, one in the sensor node and one in the readout unit. In all other respects, the sensor nodes can be similar to those used in radio-based systems. In addition, the inductive link can be used to transmit power to the wireless sensor, which can be stored in battery and used afterwards when the external power is not available. The inductive link coils in the sensor can be very small, although the maximum transferred power is limited by the coil arrangement. The reading ranges are much smaller than those of radio-based systems. A hybrid solution that uses an inductive link for power transmission and electromagnetic waves for data transfer has been tested in [19].

Conventional wireless sensor nodes are complex devices that cannot easily be miniaturized or mass-produced. RFID systems seem to offer an alternative [20]–[22]. In RFID technology, almost all of the components are integrated into a single silicon chip. There are RFID systems that have their own power source, although RFID technologies are typically regarded as passive as they utilize the power that they receive from the reader unit. By default, RFID circuits do not have sensor functions. RFID technologies can be divided into those methods that use electromagnetic waves, and those that utilize inductive coupling. Nevertheless, power consumption is a problem and the limited energy does not allow the use of complicated signal conditioning, unlike in systems that have batteries. Cook *et al*. have conducted a review of passive chip-based and chipless RFID systems [21]. The chipless RFID sensors operate at UHF frequencies. The sensing element directly modulates the impedance matching of the antenna, and thus alters the amount of energy that is reflected back to the reader device. Chip-based RFID sensing methods increase the reliability of the readouts by using digital data transmission. The chip has an ADC and it incorporates the sensor readings into the backscattered signal. Viikari *et al.* have presented an intermodulation readout principle for passive

wireless sensors [23], [24]. In this system, a wireless sensor is activated by using signals with two frequencies. The measured data is transmitted back at the corresponding intermodulation frequency.

RFID technologies that operate at HF frequencies and use inductive coupling have also been tested for sensing applications. In [25], Potyrailo *et a*l. measured humidity using the resonance antennae of inductively coupled RFID circuits. They proposed that the RFID chips can be used to identify the sensors and to store calibration data. The chip itself was not actively used for the measurements. Thus, the measurements were, in principle, similar to the set-up used in [26] where an RLC circuit was used to sense the environment.

2.3 Measurement system

The structure of the measurement system of inductively coupled passive resonance sensors has to be investigated in order to better compare the performance of the measuring methods. The most significant detail in the measuring chain is the part where the signal is transmitted over a short distance using a magnetic field. The main physical components of the system are a resonance sensor, a reader coil and a readout device (Fig. 1).

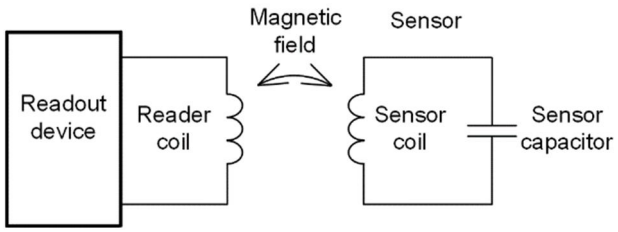

FIGURE 1. The main physical components in the studied measurement method.

A flow chart showing the information in the measurement system is shown in Fig. 2. The measurand alters the value of one of the components in the resonance sensor. The sensing element can be based on either capacitance, resistance or inductance. This part of the measuring chain is very similar to any other sensing system, and thus many conventional sensor elements can be utilized.

The changes in the sensing element alter the impedance of the resonance sensor. That impedance is detected indirectly from the reader coil. The readout device generates an excitation signal which will induce an alternating magnetic field around the reader coil. This magnetic field also extends to the sensor coil, so the resonance sensor affects the generated magnetic field. Thus, the impedance of the resonance sensor will have a frequency-dependent effect on the measurement of the reader coil, which means that changes in the measurand can be detected by measuring the impedance of the reader coil. The information is transferred from the sensor to the reader coil by the principle of inductive coupling, which is possible in the so called near-field ($x < \lambda/(2\pi)$ where x is the distance between coils and λ is wavelength [15].

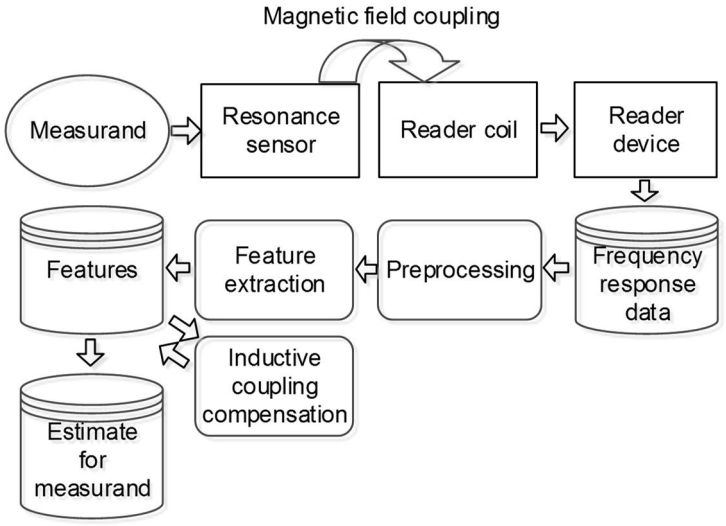

FIGURE 2. The generic flowchart of information in the investigated measurement method.

The effect of the resonance sensor on the reader coil measurement is frequency-dependent, so many readout devices make measurements at multiple discrete frequencies. This yields frequency response data. This data is preprocessed by removing the baseline curve of the reader coil. Here the baseline curve means the frequency response that would be measured in the case where there is no resonance sensor near to the reader coil. There is also the possibility of averaging the acquired values, as long as the measured quantity does not change during the measurements. Next, the feature extraction process is used to find the notable characteristics from the data. A typical feature is the frequency of a distinguishable shape in the resonance curve. The extracted feature can be used to estimate the resonance frequency of the sensor. The difference between the extracted feature and the resonance frequency of the sensor in free space is dependent on the measurement set-up. If needed, the sensor capacitance or inductance can be calculated using the resonance frequency estimate and a prior knowledge of the component values. The changes in the coupling coefficient can alter the detected frequencies [25]. In some cases, other features like the heights of the

peaks and dips in the measured data can be used to compensate for the effects caused by changes in the inductive coupling. The compensation methods are discussed in Section 2.8.

The measurement chain has many physical and signal processing stages. Understanding and optimizing the measurement systems is not always straightforward because the physical components and readout device determine the requirements for the subsequent signal processing. On the other hand, this does mean that many of the problems thrown up in the physical stages can more easily be solved in the later stages by signal processing. All of these factors have to be taken account when optimizing the measuring chain. Optimizing all stages and considering all possible options simultaneously is not realistic. Thus, the system has to be developed through iteration, focusing separately on those parts of the measuring chain that are found to be problematic.

2.4 Resonance sensors

The main structure of the inductively coupled resonance sensor is an electrical circuit consisting of a coil and a capacitor. In its physical realizations, the coil also has a detectable parasitic resistance, which manifests itself when the circuit is measured. A physical resistor can be added to the circuit if it is used as a resistive sensing element. The lumped element model representing this kind of resonance sensor is an RLC circuit (Fig. 3). Typically, one of the circuit components is variable and modified by the measured quantity.

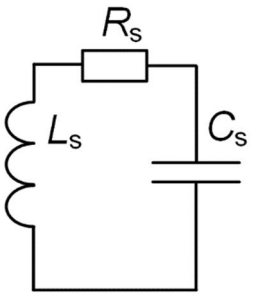

FIGURE 3. The lumped element model of an inductive coupled passive resonance sensor. One of the components is made sensitive to the measurand.

The resonance behavior of the inductively coupled passive resonance sensor can be analyzed without the readout system. At the resonance frequency, the capacitive and inductive reactances are equal but they have opposite signs and thus they cancel each other out. The impedance of the circuit is purely resistive at the resonance frequency. In such cases, the resonance frequency can be calculated with the equation,

$$f_0 = \frac{1}{2\pi\sqrt{L_s C_s}}, \quad (1)$$

where f_0 is the resonance frequency of the sensor, L_s is the inductance of the sensor and C_s is its capacitance [27].

The resistance R_s can be taken account when estimating the resonance frequency of inductively coupled RLC circuit [28], [29]. In that case, the resonance frequency is calculated with the equation,

$$f_0 = \frac{1}{2\pi}\sqrt{\frac{1}{L_s C_s} - \frac{R_s^2}{L_s^2}} \quad (2)$$

In many applications, the effect of the sensor resistance on the resonance frequency is small and can be ignored. Instead, the resistance is used to define the Q-value of the sensor

$$Q = \frac{\omega_0 L_s}{R_s}, \quad (3)$$

where ω_0 is $2\pi f_0$ [27].

2.4.1 Physical structure

The physical appearance of inductive coupled passive resonance sensors can vary depending on the components. The two most common forms of coils are helical/solenoidal and planar spiral. The solenoidal coils are made by winding the conductor wire around a supporting structure. The planar coils can be made using fabrication processes such as photolithography and thin film depositions. The same fabrication processes can also be used to make capacitors. Thus, planar coils are often preferred because all of the components can be made with similar processes, and the result is often more compact, reliable and straightforward to produce. The models of the inductance calculations for planar spiral coils have been studied in [30]. The two main ways to create capacitive structures in passive resonance sensors are parallel plate capacitors and interdigital capacitors. Parallel plate capacitors are often used in pressure-sensing applications [28], [31], [32]. The finger electrode structures are typically used when the capacitor has to sense the permittivity of the environment [33] or its moisture [34].

2.4.2 Materials

The choice of the materials used in coils, wires and electrodes depends on electrical conductivity. There is no exact lower limit for the conductivity, since the Q-value and the losses also depend on the sensor design. Copper [35], gold [28] and silver [31] have been tested as wiring and coil materials. Magnesium [36], [37] and iron [36] has been also proposed as conductor materials for biodegradable sensors. Conductive polymers have been tested by Boutry *et al*. [36], [38]. They established that polypyrrole is a possible material for inductively coupled passive resonance sensors, but it is challenging because of its poor conductivity.

Dielectric materials are needed for the capacitors and the substrates. Electrically insulating materials are also needed for the casing of the sensor. Unlike with the conductors, the quality of the isolating materials is not usually a limiting factor. However, if the sensor is to be used in liquid environments, such as with surgical implants, then the partial conductivity, and especially the dielectric losses, have to be considered. Polymers, glass or glass fibers are used as substrates and structural materials since many of the sensors' fabrication techniques are based on the ones used for printed circuit boards. Ceramic materials can be used to make inductively coupled passive resonance sensors suitable for high temperature applications [31], [39]. In biodegradable applications, polymers like polylactic acid (PLA) have been tested as substrate material and polycaprolactone (PCL) as spacer material [32]. Hwang *et al*. have proposed that silk can be used for biodegradable substrates and casings [37].

2.4.3 Measurands

In conventional sensors, the measured quantities are designed to alter the resistance, capacitance or inductance of the sensing elements. A similar approach can be applied to inductively coupled passive resonance sensors. Pressure measurement is a typical application for passive resonance sensors. The sensing is based on pressure-dependent capacitors, in which the pressure bends a membrane, or some other structure in the sensor, and thus alters the geometry of the capacitor. The sensing is based on the pressure difference across the membrane, so a reference pressure is needed on one side of the bending structure. Sealed cavities can be fabricated inside the sensor [28], [40], [41]. The reference pressure can be a vacuum, or simply the atmospheric pressure. Inductive coupled pressure sensors are a potential solution for taking measurements in many harsh environments. For example, they have been developed and tested for taking pressure measurements inside living tissue [11], [28], [42], and also in very high temperatures [31], [43].

Inductively coupled passive resonance sensors can also be used to monitor the immediate environment. This is done by designing the resonance circuit in such a way that the environment can interact

with the electric field around the sensor. In this case, the relative permittivity of the environment is monitored. The real part of relative permittivity mainly affects the capacitance of the sensor, while the imaginary part affects the losses, which can be modelled with an equivalent resistance. The effect of the environment on resonance sensors was reported by Collins as long ago as 1967 [11]. Later, Ong *et al*. measured the complex permittivity of the environment with an interdigital capacitor [26]. They also used passive resonance circuits to sense other parameters, such as temperature, growth of bacteria and humidity. In more recent studies, Zhang has investigated inductively coupled sensors for dielectric constant permittivity sensing [33], and Yvanoff has proposed the use of interdigital capacitors for tissue characterization [44]. Capacitive sensors are particularly good for measuring the humidity or the moisture content in certain materials because water has relatively large permittivity in comparison with air or structural materials. The inductive coupling means that the sensor can be placed inside the structures, or in materials such as soil or sand. Inductively coupled passive resonance sensors have successfully been tested to measure the moisture content of construction and civil engineering materials [34], [45]–[47], as well as the humidity inside containers [48]. These measurements can be enhanced by using a humidity-sensitive polymer film on top of the sensor [49]. In addition, Potyrailo *et al*. tested temperature compensation based on PCA [49] and proposed modified RFID tags for multipurpose chemical sensing to detect toxic vapors [50], [51]. Moreover, passive resonance sensors have also been tested to monitor bacteria [52], [53].

The measurand can be also be linked to the resistance in a resonance sensor. Bona *et al*. reported on the use of a resistive strain gauge as a sensing element [54]. Manoor *et al*. tested a graphene-based resistive sensing element on top of an interdigital capacitor [53], and a resistive ZnO element has been proposed to measure oxygen in high temperatures [55].

A varactor is a voltage-dependent capacitor. Varactors can be used to convert a voltage measurement to a capacitance measurement and thus enable voltage to be measured using inductively coupled passive resonance sensors. In [56], a passive resonance sensor was used to measure an ECG, and Horton *et al*. used a varactor to measure the voltage of pH electrodes [57].

2.5 Inductive coupling

The coupling between two electrical circuits can be described by their mutual inductance, *M*. The geometry of the coils, the distance and orientation between them, and the magnetic properties of the medium determine the mutual inductance. The mutual inductance between two coils cannot easily be expressed with a single equation in a generalised form because of the multitude of possible coil design options and the number of parameters required to define a 3-dimensional geometry. Thus,

separate equations have to be used for specific situations. For example, if the primary coil is much larger than the secondary coil, the mutual inductance for on-axis circular coils can be calculated by

$$M = \mu N_1 N_2 \left(\frac{\pi (r_1 r_2)^2}{2\left(x^2 + r_1^2\right)^{3/2}} \right), \tag{4}$$

where N_1 and N_2 are the number of turns of the primary and secondary coils, respectively, x is the distance between the coils, r_1 is the radius of the primary coil, r_2 is the radius of the secondary coil, and μ is the permeability [58]. Analytical calculations of the mutual inductance for coaxial rectangular spiral coils have been presented in [59], and the effects of misalignment has been studied in [60].

The coupling between two coils can be described by the inductive coupling coefficient, k. The absolute value of the coupling coefficient is between 0 and 1 and can be defined by using the mutual inductance and the inductance values of the coils,

$$k = \frac{M}{\sqrt{L_1 L_2}}, \tag{5}$$

where L_1 is the inductance of the primary coil and L_2 is the inductance of the secondary coil [27]. The coupling coefficient can be also approximated based on the distance and orientation between the coils and their geometry [15], [58].

The effect of the secondary circuit (the resonance sensor) on the primary circuit (the reader coil) can be modelled with an equivalent impedance in series with the reader coil [27]. The equivalent (or coupled) impedance is calculated by the equation

$$X = \frac{(\omega M)^2}{Z_s} \tag{6}$$

where Z_s is the series impedance of the secondary circuit and $\omega = 2\pi f$. In the case of an RLC circuit, Z_s is

$$Z_s = R_s + j\omega L_s + \frac{1}{j\omega C_s}. \tag{7}$$

Inductively coupled resonance sensors have been modelled using this concept in [40], [56] and a similar model has been tested in [26].

2.6 Readout devices

Inductively coupled sensors are monitored by measuring the properties of the reader coil using so-called readout devices (see Fig. 1). Typically, this can be done by feeding excitation energy to the coil and measuring the response. This response can be, for example, the voltage over the reader coil. The responses are modified by the impedance of the reader coil and the reflected impedance of the resonance sensor. The readout methods can be categorized based on the type and frequency of the excitation signal. A readout device can operate using a single frequency. For example, this can be done using an envelope detector and a sinusoidal excitation signal at the set frequency [56]. In addition, there are methods where the excitation signal is adjusted to the resonance frequency using phase-locked detectors [56]. Neither of these readout schemes necessarily requires further signal processing, because the analog outputs of the devices can be linked to the resonance frequency of the sensor. These methods can also capture rapid changes in the frequency of the resonance sensor. However, the effects of the changes in inductive coupling, or the effects of the Q-factor, remain unknown in these methods. One problem with the envelope detector method is that the excitation signal has to be in the right range in comparison with the resonance frequency of the measured sensor. The frequency range in which a phase-locked system can lock on to the resonance frequency of the sensor is also limited. There are also readout methods where the sensor is first activated to resonate by using an excitation signal burst. Afterwards, a decaying response signal can be detected [13], [61].

Readout methods are more often based on frequency sweeps. Collins used a device based on grid-dip oscillators to measure inductively coupled passive resonance sensors [11]. In this method, the energy absorption of an LC sensor was measured. The frequency of the excitation signal in this system was adjustable and constantly altered within a certain range. This allowed the absorption to be measured as a function of frequency [11]. Alternatively, instead of the continuous sweeps used by Collins, the responses can be measured at fixed frequencies, which seems like a more intuitive approach in modern systems that process digital data.

2.6.1 Commercial measurement devices

Inductively coupled passive resonance sensors are often measured using commercial impedance analyzers [26], [28], [31], [32] or network analyzers [35], [38], [62]. These devices measure electrical

parameters at set frequencies. The devices have large and adjustable frequency ranges and fast measurement rate. The disadvantages of these devices are that they are bulky, expensive laboratory devices and they are not designed to be used in a more demanding environment. The impedance analyzers can use the I-V method [63], [64] to measure complex impedances. The basic concept behind this method is to measure two complex quantities: the current passing through, and the voltage over, the unknown component. The excitation current is typically created by letting a voltage force a current through a known impedance and tested circuitry. Then the voltage over the known impedance can be determined, which allows the current that is fed to the tested circuit to be calculated. The unknown impedance of the tested circuitry can then be calculated using Ohm's law. The implementation of this measurement concept can vary and the actual measurement circuitries are more complicated than suggested by the basic concept [64]. The impedance analyzer can also made be made more compact [65]. In the network analyzer method, the unknown impedance can be calculated from a reflection coefficient measurement that is based on measuring incident and reflected signals [64]. Both measurement methods yield frequency sweep data, which means that a signal processing stage is needed in order to estimate resonance characteristics, such as the resonance frequency.

2.6.2 Custom-made readout devices

Commercial impedance and network analyzers are general measurement devices rather than dedicated readout devices for inductively coupled sensors. Various dedicated readout set-ups and devices have been tested. Coosemas *et al*. proposed readout electronic circuitry where a voltage-controlled oscillator performed frequency sweeps, and the voltage across the external coil was monitored [29]. They used an envelope detector to demodulate high frequency signals. The main benefit of this approach is the simple and low-cost detector circuit. Pichorim *et al*. have presented a system that is based on three simultaneous excitation signals at different frequencies [66]. This method includes three coils for the readout and one coil in the sensor. Their method allows the calculation of the resonance frequency and a quality factor. Nopper *et al*. proposed a readout method that consists of an analog front end and a digital signal processing unit [67], [68]. The output signal of the front end is proportional to the real part of the measured impedance. The frequency of the excitation signal is continuously readjusted by the digital signal-processing unit. By using these modules, the system was able to detect an estimate for the resonance frequency. In [69], Sardini *et al*. proposed a custom-made device that measures both the real and imaginary parts of the admittance. Their device included a direct digital synthesizer, three analog multipliers for down-mixing high frequency input, a microcontroller and an analog-to-digital converter. Their data was processed in a PC and they verified the operation of their device against a commercial impedance analyzer. There are also

examples of portable custom-made readout devices. Voutilainen tested a hand-held device to measure humidity sensors in the field [47].

2.7 Signal processing

The form of the processed data

Signal processing is often needed to extract the resonance characteristics from the measured data. The details of this procedure are dependent on the readout device and measured data. In the case of impedance and network analyzers, the result of a single frequency sweep yields a vector containing quantity values at the preset frequencies. The measured quantities are the real or imaginary parts of the impedance [26], [46], [57], [70] or the phase of the impedance [28], [32], [40]. The quantity in the network analyzer measurements is typically the S_{11} parameter [35], [38]. The S_{11} parameter is one of the scattering parameters and describes the input port voltage-reflection coefficient.

The presence of the resonance sensor near to the reader coil will alter the measured values and causes a resonance curve to appear in the data. The shapes of these curves vary. The position of the resonance curve in the frequency axis is mainly determined by the resonance frequency of the sensor, but it can be slightly modified by other factors, such as the coupling coefficient. The width and height of the resonance curve are affected by the losses in the sensor and the coupling coefficient.

Pre-processing

The reader coil will also affect the measured values. Since this effect mainly stays constant, the baseline can be measured and removed before the actual feature extraction takes place [26], [28]. Removing the baseline of the reader coil will make the resonance curve stand out, which is more amenable to further signal processing. This can be critical when the inductive coupling is very weak and the resonance curve is hard to detect. If the measurand is considered to be constant during the measurements, averaging the measured signals before they are processed any further reduces the effects of random noise [28].

Extracted features

The features can be used to characterize the resonance curve. They can be used to estimate the resonance frequency of the sensor, the losses, or the coupling coefficient. Because the measured data and the resonance curves vary, there are many possible features that can be extracted. For

example, the frequency of the maximum in the real part of the impedance has been estimated in [26], [70]. In this thesis, the estimate for this frequency is referred as f_{max}. Another often-used feature is the frequency of the minimum in the phase of the impedance [28], [32]. This feature is sometimes referred to in the literature as the phase-dip method [67]. The estimate for this frequency is referred as f_p in this thesis. These features are believed to bear a strong correlation with the resonance frequency of the sensor. The zero-reactance frequency [26] and resonant and anti-resonant frequencies of the imaginary part of the impedance spectrum have been also used as features [70]. Moreover, Marioli *et al*. evaluated three resonance frequencies from the magnitude of the impedance [71]. In general, the commercial devices express the measured impedance either in Cartesian or polar forms. The features have been evaluated from the measured curves as the frequencies of notable shapes. Typically, a tested feature is either a local maximum (a peak) or a local minimum (a dip) in the curve. In the case of network analyzer measurements, the detected form has been a dip in the curve [35], [38]. As an alternative approach, parameter estimation can be used to find resonance characteristics [31].

The width of the resonance curve can be linked with the losses in the resonance sensor, and especially with the losses in the resistance of the sensor circuit. The features used to correlate with the losses are either the bandwidth of the resonance curve or the Q value [31]. In contrast, the height or magnitude of the resonance curve correlates with the coupling coefficient. For example, the maximum of the real part of the impedance has been extracted [25].

2.8 Inductive coupling compensation methods

Any variation in the inductive coupling affects the shape and position of the measurable resonance curves. Thus, it is natural to assume that inductive coupling also affects the resonance frequency estimates. Typically, inductive coupling is subject to changes in the position, angle or alignment between the reader and sensor coils. The most obvious effect is the variation of the height of the resonance curve due to the changing inductive coupling. The significance of errors due to the changes in inductive coupling depends on the measurement set-up. In some cases, the error is assumed to be insignificant if the inductive coupling coefficient is estimated to be small [32]. The problem caused by the changes in the inductive coupling was mentioned by Collins as long ago as 1967 [11]. There are a number of articles that discuss compensation methods for this [25], [71]–[73], and it is clear that errors due to changes in the inductive coupling and the corresponding compensation methods are topics that have to be addressed.

The information about the height of the resonance curve can be used to compensate for the changes in the resonance frequency estimate. For example, Potyrailo *et al*. used Principal Component Analysis (PCA) to diminish the effects of the inductive coupling on the measurement [25]. One of the features used in PCA was the maximum of the real part of the impedance. The other features were the frequencies identified from the real and imaginary parts of the impedance. The results showed that one of the estimated principal components correlated well with the measured quantity and, in addition, the changes in the positioning between the used coils did not have a significant effect on this component [25]

Marioli *et al*. have proposed a compensation system where three noticeable frequencies are identified from the magnitude of the impedance [71]. They stated that two of the frequencies are dependent on the sensor while one is dependent on the self-resonance frequency of the reader coil. They were also able to derive a compensation parameter based on these three frequencies. The sensor's capacitance was then calculated using the compensation parameter, one of the identified frequencies and the constants. This method was later applied to humidity measurements in which the distance was varied [72].

3 Readout methods

This chapter presents the readout methods that were developed and tested to improve the feasibility and accuracy of inductively coupled passive resonance sensors. These methods consist of the readout device, feature extraction methods, and a method for compensating for the effects of changes in the inductive coupling.

3.1 Custom-made readout device

The performance of a readout device can be the limiting component in any measuring chain and this problem has hindered the use and applicability of inductively coupled passive resonance sensors in the past. Although readout methods such as envelope detectors and phase-locked readout devices enable fast measurements [56], [74], these devices can only operate within a rather narrow frequency range without the need to adjust or retune the measurement system. This restricts the choices in sensor design and requires low manufacturing tolerances. A narrow frequency range also limits the dynamic range of the sensor. Impedance and network analyzers, on the other hand, have wide and adjustable operating ranges. The major problems with these devices are that they are often stationary and expensive laboratory devices and the measured target and the sensors have to be brought to the readout device, rather than vice versa. This is obviously not possible for many applications. In addition, the memory and the data transfer methods of these devices often seriously constrain the use of continuous high frequency sampling.

In order to counter the problems of the existing readout systems, a custom-made readout device was designed specifically to promote the development of inductively coupled passive resonance sensors. The original design objectives were its feasibility and sampling speed. In addition, the device would have to be easy to configure and optimize for a range of different sensors. The general applicability of this measurement system will lead to more testing and more data, which in turn promotes faster sensor prototyping and iteration. Secondly, the device should be portable to allow testing in applications where bulky laboratory instruments are not a feasible option. Thus, our prototype readout device was implemented using a simplified version of the method used in conventional impedance analyzers. A schematic of our custom-made readout device is shown in Fig. 4a. The hardware of the measurement system was implemented as a USB-device (Fig. 4b) that can be connected to a laptop computer for post-processing. The electrical operation of the device is explained in detail in [P1].

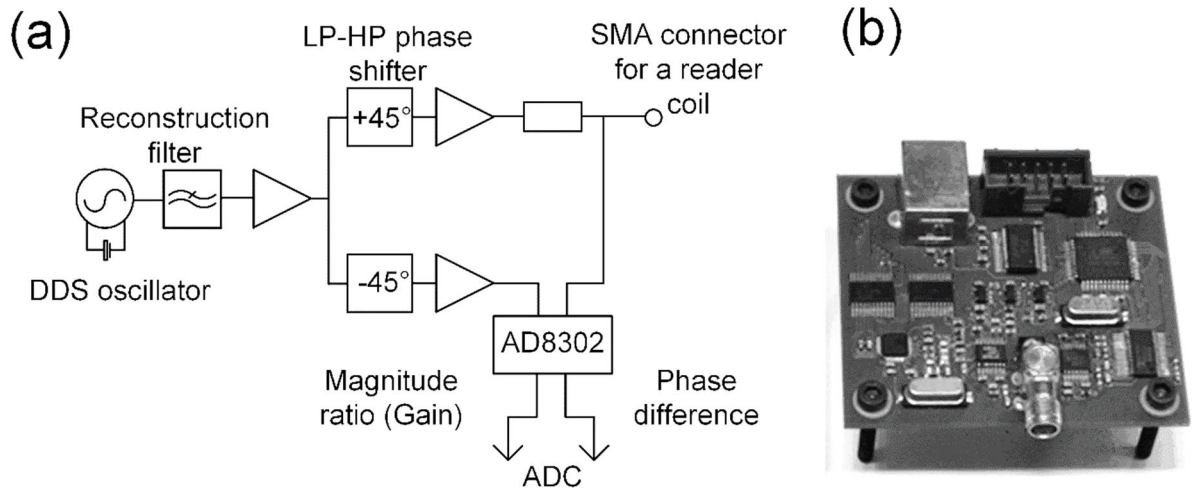

FIGURE 4. a) A simplified schematic of the custom-made readout device. b) The first prototype of the custom-made readout device.

This readout device takes measurements at preset frequencies, as does an impedance analyzer. However, instead of a real impedance measurement where the complex current and voltage are measured, this device merely measures the gain/magnitude ratio and phase difference of the voltage against a reference channel with an AD8302 detector circuit (Analog Devices) [75]. This means that our measured values differ from the values measured with a calibrated impedance analyzer. The voltage is measured after a serial resistor, which is used to transmit the excitation signal to the reader coil. The device allows fast frequency response measurements that can be used to estimate the resonance frequency of the sensor. This is possible because accurate measurement of true impedance is not always needed when the measurement is based on the change of the resonance frequency of the sensor.

The software of the device was designed to allow the customization and optimization of the frequency sweep parameters. These parameters have to be adjusted based on the tested sensor. In a typical application, the measured quantity is linked to the sensor capacitance, whose variation defines the required frequency range. It is important to ensure that the whole resonance curve is within the measured range. For this reason, the software previews the measured data. The selection of the frequency sweep parameters, such as the frequency range and the number of data points, is an optimization problem. The measurement of each data point takes a set amount of time. Therefore, a frequency sweep that has a minimum number of data points is optimal for fast measurements. On the one hand, there has to be enough data points to estimate the features in the data. In contrast to some commercial devices, the software provides a direct and fast interface to the measured raw data.

3.2 Signal processing

The data measured with the custom-made readout device consists of frequency sweeps. If there is a sensor near the reader coil, a specific resonance curve can be found in the measured data (Fig. 5). The shapes of the measured curves vary depending on the measured quantity and the measurement set-up. The measurement set-up comprehends the resonance sensor, the reader coil and its parallel capacitances (such as a cable), and the inductive coupling between the coils. The reader coil, its parallel capacitances and the used readout device affect the baseline of the measurement. In this work, the tested applications were a wireless pressure measurement, monitoring the condition of ceramic slurry during its production, and monitoring biodegradable polymers during hydrolysis. The phase difference between two channels was measured in both the pressure garment and polymer monitoring applications, while the voltage gain between the channels was measured in the slurry fabrication application. Based on the operation principle of the AD8302 it was assumed that phase data would give a better signal-to-noise ratio. Thus the measurement of phase curve was preferred, however in suspension monitoring application the shape of the gain curve suited better for estimating

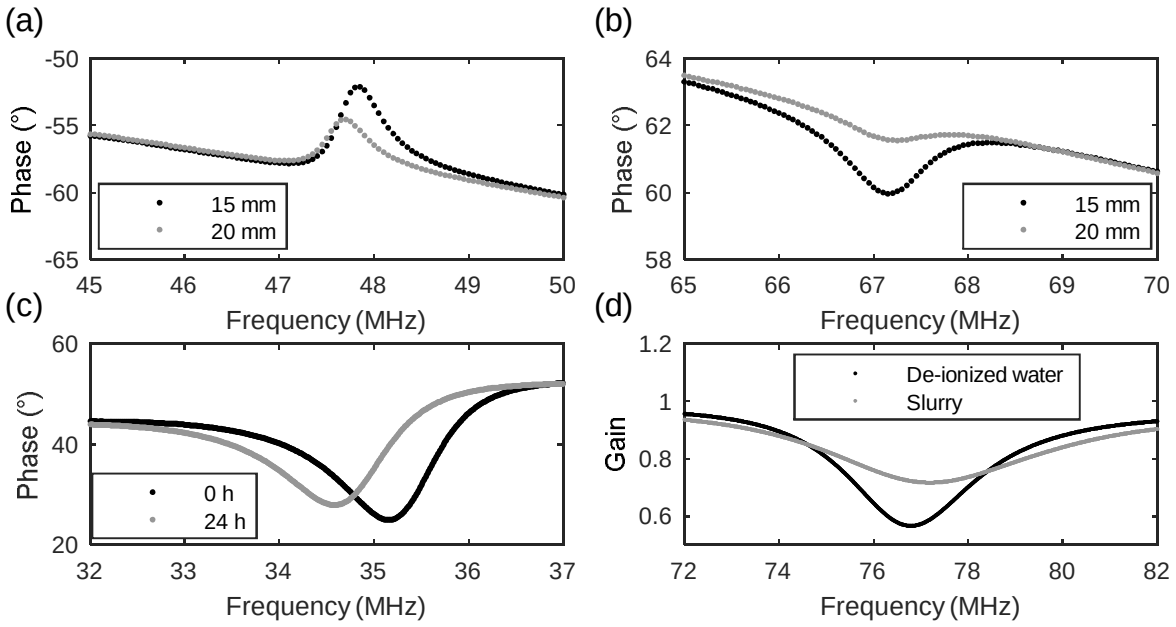

FIGURE 5. a) Resonance curves of a pressure sensor measured using a large reader coil in [P1], b) resonance curves of the pressure sensor tested in [P2], c) resonance curves measured in the polymer degradation measurement, and d) the resonance curves measured in the slurry monitoring application [P4].

the losses in the measured resonance sensor. Each application had specifically designed inductively coupled sensors and specific measurement set-ups. Fig. 5a shows the resonance curves of the first pressure sensor we developed measured from two distances using a large multi-turn coil. Figure 5b illustrates the resonance curves that were measured from two distances using a small, single-turn reader coil. The resonance curves measured in the polymer degradation experiment at the beginning of the experiment and after one day are shown in the figure 5c, while Fig. 5d shows typical measurement results (wide dips) acquired in the slurry monitoring application.

3.2.1 Feature extraction methods

The examples in Fig. 5 show that the measured response curves have different shapes depending on the measurement set-up. Feature extraction methods were used to characterize these curves. The idea behind this methodology is to compress the measured frequency sweep data into features that give information about the resonance sensor or the inductive coupling. In an optimal situation, each feature would only be dependent on one component in the measurement system, but this cannot always be achieved. The signal processing methods should also be able to handle situations where the size, shape or position of the resonance curves are significantly altered due to changes in the measurement set-up.

The measured data contains distinguishable peaks and dips. The frequency of these shapes can be extracted from the data as frequency-valued features. These features can be used as an estimate for the resonance frequency of the sensor. However, the values of these features are not necessarily the same as the resonance frequency of the sensor in free space (f_0). Two other features were also extracted. Inductive coupling affects the height of the resonance curves, so this was one feature to extract. In addition, the losses in the sensor not only affect the height of the resonance curves, but they also make them wider, so the widths of the resonance curves were also estimated in some cases.

The feature extraction methods for the data measured with the custom-made readout device were developed and tested in [P1], [P2], [P4] and [P5]. The details of the extraction process varied and evolved over time, but the overall process flow for finding features remained broadly the same. The generalized feature extraction algorithm consists of the following steps:

1. Remove the baseline.
2. Find the data point with a maximum or minimum value from the measured data.
3. Select data points around the detected maximum or minimum.
4. Fit a polynomial model to the selected data.
5. Evaluate the frequency of the maximum or minimum by using the polynomial model.
6. Evaluate the value of the maximum or minimum (optional).
7. Evaluate the width of the resonance curve by using the model (optional).

The baseline was subtracted from the data to make the peak or dip stand out. An example figure that illustrates this operation is given in [P4, Fig. 3]. Similar approaches have been taken in [26], [28]. Some examples of the resonance curves after this procedure are given in Fig. 6. A data point with a maximum or minimum value was detected from the frequency sweep data. Next, the essential part of the measured data around the found minimum or maximum was selected, and then a polynomial regression model was fitted to that data. Third-order polynomial models were used to take into account the asymmetry of the measured shapes. This allowed an estimate for the frequency of the shape (a peak or a dip) to be interpolated.

Only a section of the measured data vector was used to make the regression model because the range of the measured frequency sweeps was relatively wide in comparison with the actual resonance curve. The shapes of the measured curves are intricate, so simple models are only suitable for a limited range in the neighborhood of the peaks or dips. The rules for selecting the modelled data points were thus adjusted according to the measured data. In [P1], [P2], [P4] and [P5], the value of the selected points was a certain percentage of the value of the maximum or minimum. In the simulated data in [M1] and its verification measurements, 15 points around the found maximum or minimum were selected to ensure that all the models had the same number of data points (the figures 6c and 6d). Another advantage of this method is that, since the model is based on a set of measured samples, the extraction process of the resonance frequency estimate is less prone to noise from a single measurement.

The regression model was also used to estimate the value of the local maximum or local minimum. These estimates were used to calculate the height of the curve, which in turn were used for the inductive coupling compensation. If the resonance curve had a detectable peak and dip, the height was calculated by subtracting the value of the local minimum from the value of the local maximum; otherwise an absolute value of the measured quantity at the frequency of the dip was used (Fig. 6d). If the application required monitoring the losses in the resonance sensor, the width of the peak or dip was estimated using the model. The difference between the frequencies, when the value of the model was 70.7 % of the minimum (or maximum), was regarded as being the width. An example of this procedure is given in [P4].

The tested features

The feature extraction methods were applied to the measured and simulated data. Examples of that data and the extracted features are given in Fig. 6. The shapes of the measured resonance curves were specific to each tested application because the acquired data depicts the characteristics of the combined measurement set-up, rather than just the sensor. Thus, a set of features were tested to characterize the curves measured with our readout device.

In [P1], the most distinguishable shape in the measured phase data was a peak, so the frequency of the maximum (f_{mu}) of the peak was extracted (Fig. 6a). In the data measured in [P2] and [P5], there was a dip in the phase data, so the frequency of the dip (f_{md}) was extracted. The feature f_{md} was also estimated from the simulated data that approximates the measurement set-up in [P2]. These curves are shown in Fig. 6b, 6e and 6d, respectively.

A secondary shape before the dominant shape (either a dip or a peak) was modelled in the compression garment applications as seen in the figures 6a and 6b. In the simulated data shown in Fig. 6c, the resonance curve has two detectable shapes: a dip and a peak, both of which were modelled.

To find out the height of the shapes, the values of the local maximum (Θ_u) and local minimum (Θ_d) in the phase curves were calculated using polynomial models. These values were used to calculate the total height of the shape induced by the resonance sensor. This height (Θ_m) was defined as the difference between the local maximum and the local minimum values.

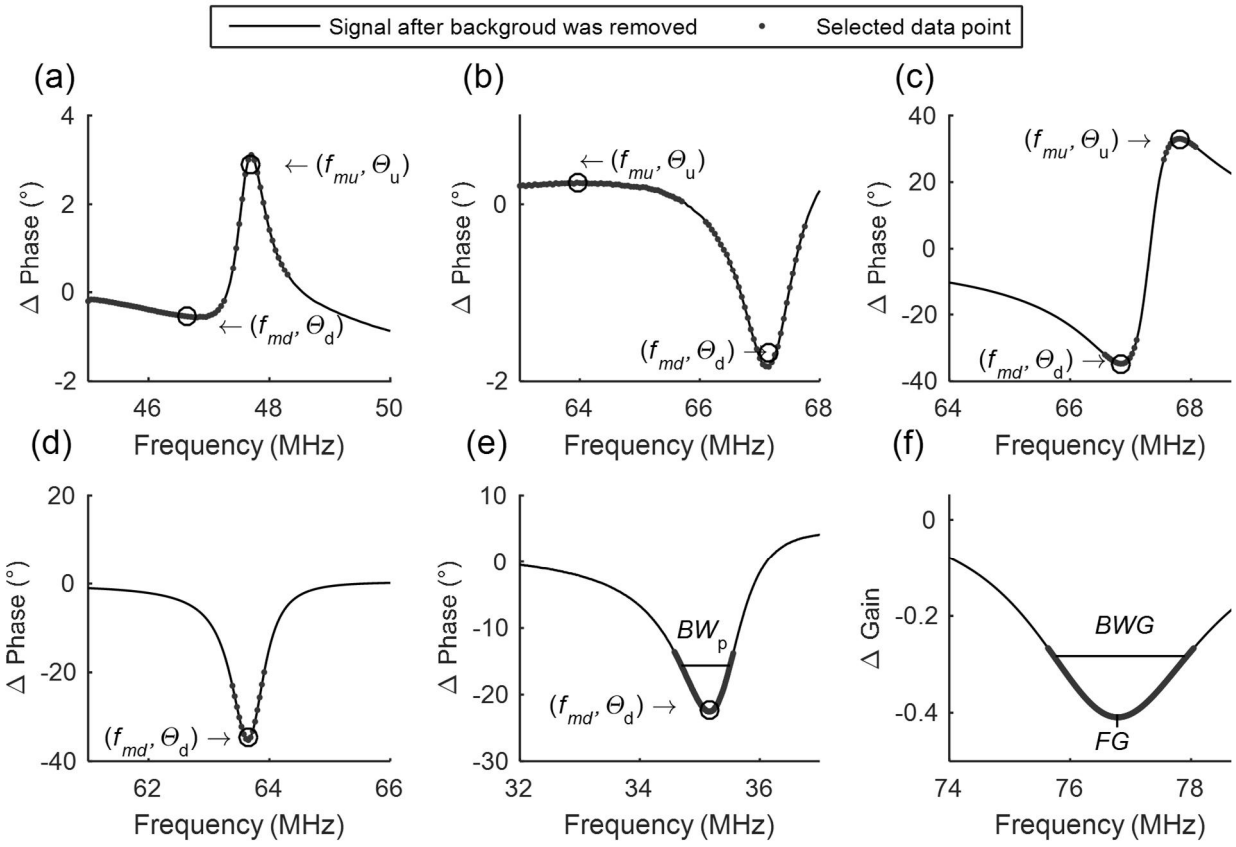

FIGURE 6. The features used to characterize the measured or simulated resonance curves.

The voltage gain measurement (Fig. 6f) was utilized in [P4] because the shape of the measured curve was more suitable for defining its width using a polynomial model. In that case, the extracted features were the frequency of the minimum (*FG*) and the width of the dip in the gain curve (*BWG*). A similar approach was used in [P5], but there the features were extracted from the phase difference curve. In this case, the feature BW_p estimates the width of the dip in the phase curve (Fig. 6e).

3.2.2 Compensation for an unknown inductive coupling

The values of the features (f_{mu}, f_{md} and *FG*) are dependent on the resonance sensor, the measurement circuitry and the inductive coupling. These features can be used to approximate the resonance frequency of the sensor (f_0). The difference between f_0 and a selected feature varies if the inductive coupling is altered during the measurement. In practice, this means that changes in the reading distance and the angle between the coils cause measurement errors. Changes in the inductive coupling also affect the relative size of the measured resonance curves (the figures 5a and 5b). Thus, the height of the resonance curve can be used to compensate for any changes in the inductive coupling.

The compensation method was based on a tuning procedure where the dependency between the features f_{mu} or f_{md} and the feature Θ_m were measured, while the inductive coupling was varied and the measurand was kept constant. An example of the extracted data is given in Fig. 7. The relation was approximated to be linear ($f_{md} = p_1\Theta_m+p_2$) but only within a limited range. The data points that had a height (Θ_m) within this range were used to create a linear regression model. The lower limit was set in order to remove uncertain data points where the resonance curve was barely detectable. The coefficient of this model (p_1) can be used to compensate for the changes in the inductive coupling in the actual measurements. The compensated resonance frequency estimate f_c was calculated for the feature f_{md} using

$$f_c = f_{md} - p_1\,\Theta_m. \tag{8}$$

A similar compensation process can be applied for the feature f_{mu} and an example of this is given in [P1].

3.2.3 Testing of the compensation method

The compensation method was tested in [P2]. The tuning procedure was concluded using a resonance circuit. The initial capacitor in this circuit was 22 pF. The tuning data was collected while the distance between the coils was varied from 1 mm to 25 mm. This yielded a set of extracted features (f_{md} and Θ_m). This data is shown in Fig. 7 (uppermost data set). Unfortunately, the dependency between these features is not totally linear within this range. Thus, only the data points having θ_m between 3 to 25 degrees were used to create the linear model. Then, discrete 0.5 pF capacitors ware added in parallel with the initial 22 pF capacitor to change the capacitance of the resonator from 22 pF to 23.5 pF in steps of 0.5 pF. This mimics the changes of the measurand in the actual sensors. The resonance circuit was measured in a similar way as was done in the tuning process after each increment. Thus, the available data consist of four data sets. This data was used to calculate values for the compensated resonance frequency estimates f_c. The average of these values

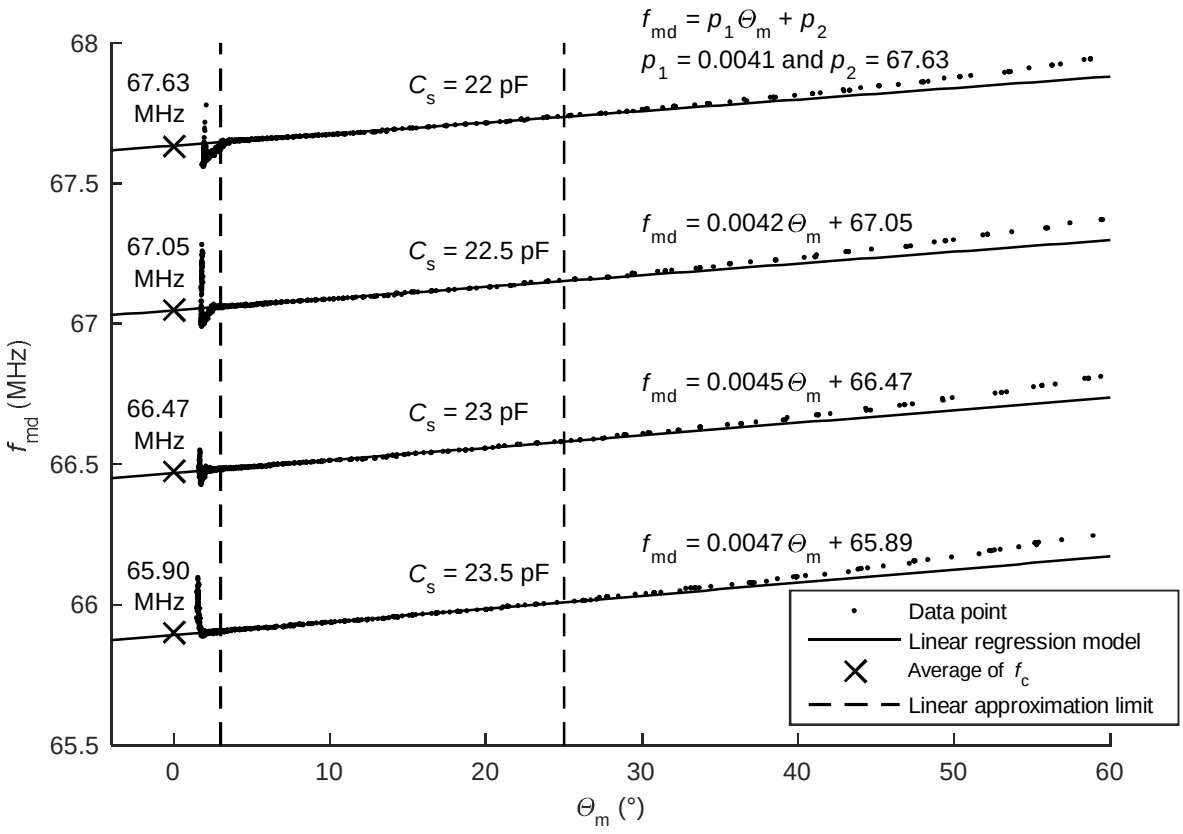

FIGURE 7. The test data of the inductive coupling compensation method. The features f_{md} and Θ_m were extracted from the data in which the inductive coupling was varied. This was done with a resonance circuit whose capacitance was altered between the measurements.

is shown in Fig. 7. In addition to the original tuning process, linear regression models were calculated for each data set within the valid range. The slope of the regression models appears to increase as the resonance frequency of the circuit decreases. This may limit the use of this compensation method, especially in those cases where the resonance frequency of the sensor deviates significantly from the initial frequency.

The performance of the compensation method was further studied by investigating the distribution of the compensated resonance frequency estimates. The differences between each compensated value f_c and the best available estimate for the corresponding resonance frequency were studied in two extreme cases. In this experiment, the values of p_2 of each data set were used as the best

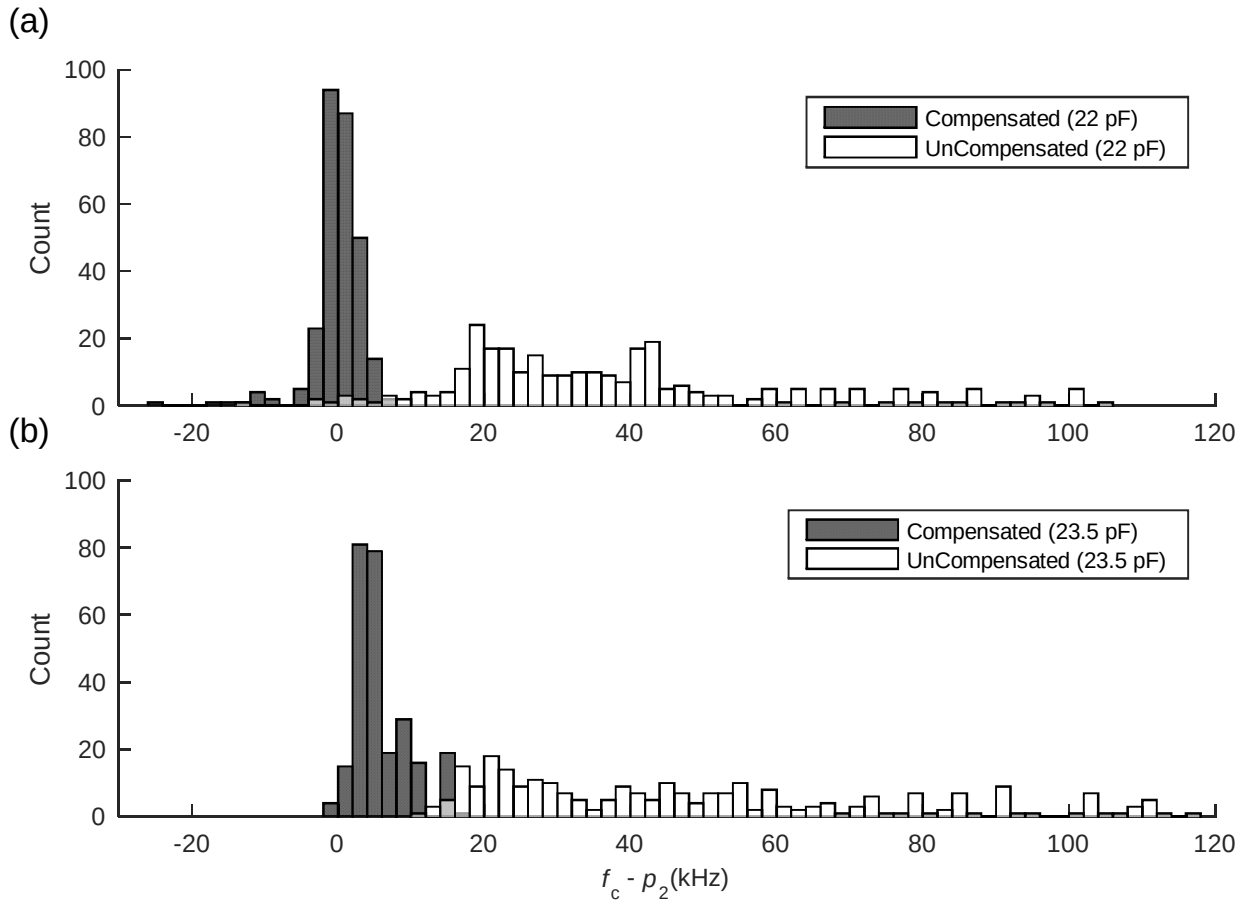

FIGURE 8. The histogram of the difference between each compensated value (f_c) and the coefficient p_2 of the corresponding data set. a) Data set measured in the situation where the parameter used in the compensation method was defined and b) in the situation where the resonance frequency of the sensor was altered from this point.

available estimate for the resonance frequency. In the first case (C_s = 22pF), the data was measured during the tuning procedure and consisted of 285 valid data points. In the second case, the capacitance of the sensor was 23.5 pF, and the data had 263 valid points. In this latter case, the values of f_c were calculated by using p_1 from the first case. This imitates the situation where the tuning data for the measurements is acquired by keeping the measurand constant and afterwards the acquired p_1 is used to compensate for the changes in the inductive coupling. A histogram of the differences in the first case is illustrated in Fig. 8a. The standard deviation of the f_c was 3.4 kHz. The histogram also shows the difference between the uncompensated feature f_{md} and $p_{2,}$ in order to demonstrate the usefulness of the compensation method. The method clearly reduces the effect of the inductive coupling on the extracted resonance frequency estimates. Fig. 8b shows a similar histogram for the second case, in which the method still effectively reduces the effect of the inductive coupling. The standard deviation of the f_c was 3.7 kHz. In this case, however, the average of f_c was 5.9 kHz higher than the value that would have been achieved if the p_1 from the second case had been used in the compensation. Thus, the compensation creates an error when the resonance frequency of the sensor moves far away from the frequency where the tuning procedure was carried out.

3.3 Discussion on the readout methods

A custom-made device was developed to measure inductively coupled passive resonance sensors. Although this approach has pros and cons in comparison with the more commonly used approaches, which utilizes commercial impedance or network analyzers, our device already has the required functionality to be used as an effective tool for monitoring the resonance characteristics of inductively coupled passive resonance sensors. The usability and robustness of the device meant that the sensors could be tested in applications where laboratory devices would have been impractical. In [P1] and [P2], a hand-held readout device allowed measurements to be taken in an application where the sensors were measured underneath clothing without using wiring or tubes. In [P4], the readout device was able to measure slurry fabrication in a dirty environment that would most definitely not have been suitable for delicate RF-instruments. Unlike impedance analyzers, our custom-made readout device does not measure the true complex impedance. Instead, it measures voltage gain and phase difference. These quantities are modulated by the complex impedance of the reader coil and the inductively coupled sensor. When the inductively coupled sensors were measured, the shapes of the curves clearly differed from the impedance measurements [76]. In [P1] and [P2], it was not necessary to take accurate measurements of the true complex impedance because the important information was coupled with the change of the resonance frequency of the sensor, rather than with the accuracy of the impedance readings. Our readout device is, of course, only one of many possible approaches, but it can be optimized much further. For example, it has already proved itself in an

application where fast sampling speed was needed [77]. If this measurement method can be developed further, or commercialized, then the opportunities offered by using such a simple readout device will be of immense importance.

The signal processing methods had to be developed to extract features from the data measured with our readout device. This data includes frequency sweeps, i.e. vectors containing the measured values of voltage gain and phase difference between two channels at the set frequencies. The resonance sensor will appear as a distinctive curve in the measured frequency responses, and the measurand alters the shape and place of this curve. Since the frequency sweeps are done at discrete frequencies, and each measurement takes time, estimates for the resonance frequencies were achieved through interpolation and not by making more dense frequency sweeps. Polynomial models were used to estimate the frequency of the peaks and dips within a selected part of the measured resonance curve. An alternative approach would have been to make parameter estimations, as Fonseca did for the impedance phase data in [31]. However, parameter estimation requires a good model for the whole measurement set-up, in addition to which, the speed and success of the estimation is highly dependent on the initial values. Because of the diversity of the measurement data provided by our device, the decision to use polynomial models was judged to be faster and to require far less a priori information about the system.

Selecting the modelled part of the curve is not straightforward. Indeed, it was not possible to use the same procedure and the same limit values for all the tested cases. Although polynomial models are not ideal for estimating the complex shapes of the resonance curves, they do have the virtues of being simple and easily adjustable, which makes them a good compromise. The tested models worked fine if they were used for interpolating the frequencies of the peaks or dips. The polynomial models also allowed the heights of the resonance curves to be calculated. A drawback with the polynomial models is that there is a tendency to underestimate the value of the measured quantity at the maximum frequency, especially if the modelled part of the curve is too long.

A compensation method was created to mitigate the ambiguity in the measurements arising from the unknown and varying inductive coupling. The method was tested in practice [P1] [P2], and it has been shown that it significantly reduces the ambiguity caused by the varying inductive coupling. The compensation method is based on the assumption that the relation between the height of the resonance curve and the extracted frequency value is linear. Based on the measured data, it seems that this approximation is only adequate within a limited range, although in practice, this range is wide enough for many applications. Furthermore, the compensation method can be, and is being, improved. For example, Deluthault *et al*. tested a modified version of the algorithm from [P1], and have suggested alternative features to improve the compensation method [78].

In conclusion, the readout methods presented here provide a tried and tested alternative method to acquire and process data from inductively coupled passive resonance sensors. This method enables processes to be monitored and measurements to be taken in completely new applications. The measurement system is a collection of physical and software components, and the overall performance of the system is, of course, dependent on their compatibility. It is not realistic to be able to optimize all the components at once, so some compromises have had to be made. Nevertheless, the present implementation is robust and straightforward, and the readout device and its signal processing are very adaptable.

4 Simulation of the readout methods

4.1 Motivation and goals

Modelling and simulations were used to study the various readout methods and to understand the acquired measurement results. Hence, the operation of the inductively coupled passive resonance sensors was modelled in [P3] and [M1]. The purpose of the modelling in this thesis was to study the problems arising from the inductive coupling and the reader coil configuration. In addition, the model was used to investigate how the sensor capacitance and resistance affected the measured resonance curves and thus, the extracted features. The model allowed comparing different readout options in the same measurement set-up.

4.2 Lumped element model

A lumped element model (Fig. 9) was used to simulate the operating principle of the custom-made readout device and impedance analyzers. This model assumes that the sensor can be modelled as an RLC circuit and that the measurement is based on the I-V method, which is used in impedance analyzers [63]. The inductive coupling was modelled using the equations given in [27]. The lumped element model, and its application for the impedance measurements, are explained in more detail in [M1]. In the literature, similar lumped element models and analytical formulas have been created to understand the operating principle of inductively coupled resonance measurement systems [26], [31], [74], [79], [80].

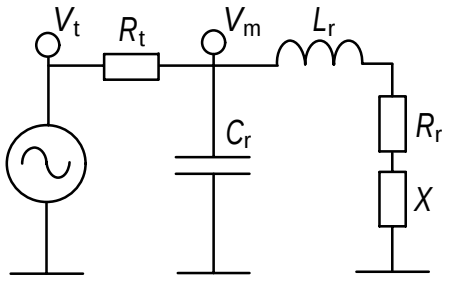

FIGURE 9. The lumped element model used in simulations.

The aim of the tested model was to capture those characteristics of a measurement system that are obvious when measured data is examined, such as the variations in the measured resonance curves

due to changes in the inductive coupling. The model is used to generate frequency sweep data that is similar to the data measured with actual measurement devices. The model does not take into account many non-idealities that are present in the custom-made readout device, such as the inaccuracy in the phase-shift circuitry or the parasitic components inside the device. Neither were the geometry of the coil set-ups or, the true mutual inductance modeled. Instead, the coupling coefficient was varied within a limited range. It was also assumed that the dimensions of the circuit are much smaller than the wavelength of the electromagnetic interrogation signal used. This, and the increasing significance of the parasitic components, decrease the performance of this model if the operation frequency is increased.

Fig. 9 shows the simplified lumped element model for an inductively coupled passive resonance sensor measurement. The reader coil and the sensor are inductively coupled. The resonance sensor was modelled as a coupled impedance, X, in series with the reader coil, L_r. The impedance X was calculated with equation (6). This equation includes the mutual inductance, M, and the impedance of the sensor, Z_s. The mutual inductance was modelled using equation (5), and by assigning values between 0 and 1 for the coupling coefficient, k. This simplification means that the model will not take into account if all the k values are possible using real physical coils. The impedance of the sensor was modelled with the inductance (L_s), capacitance (C_s) and resistance (R_s) using equation (7).

The model also contains an ideal voltage source (V_t). The resistance, (R_t), models the impedance of the component that is used to feed the current to the reader coil. The parasitic components of the reader coil (C_r and R_r) were added in order to make model valid at high frequencies (HF and VHF bands), which is where most inductively coupled sensors operate. Thus, the reader coil configuration is defined with the components L_r, C_r and R_r. The inductances of the coils were estimated with the methods presented in [30]. The parallel capacitances of the reader coils were modelled based on the measurement made with the physical coils. In the tested model, the series configuration of the components R_r, L_r and X are in parallel with the capacitor C_r. This configuration turned out to be important when modeling the effects of the inductive coupling. The magnitude and phase of voltage V_m were solved at the selected frequencies to approximate the frequency sweeps of the custom-made readout device.

4.3 Simulations

The lumped element model allows simulating the operation of the readout devices. The emphasis of simulations presented in this text was to study the operation principle of the custom-made readout device. The effects of the inductive coupling, the reader coil configuration and the sensor circuit parameters on the measured resonance curves and the extracted features was simulated. In [M1], on the other hand, the simulations were used to compare the performance of several readout methods with each other. First, the effect of the reader coil configuration on the shape of the resonance curves was studied and illustrated in situations where the inductive coupling coefficient was varied. Next, the compensation method presented in [P1] and [P2] was investigated using simulated data. Finally, the relations between the extracted features and the sensor capacitance and resistance were studied.

4.3.1 Effects of the reader coil configurations

The reader coil has a significant effect on the measured resonance curves. This has been mentioned in the literature [80] and the phenomenon can be noticed for example comparing the results measured in [P1] and [P2]. One of the most important factors for affecting the shape of the curves is the self-resonance frequency of the reader coil (f_{Lr}) and its relation to the resonance frequency of the sensor circuit (f_0). This phenomenon was studied in [M1] and three of the simulated cases are presented here (Case 1, Case 4 and Case 5). In Case 1, the resonance frequency of the reader coil (332 MHz) is much higher than the resonance frequency of the sensor (f_0 = 63.6 MHz). In Case 4, the self-resonance frequency of the reader coil (87 MHz) is above the resonance frequency of the sensor. In Case 5, the self-resonance frequency (39 MHz) is lower than the resonance frequency of the sensor. The simulated magnitudes and phases of V_m are shown in Fig. 10.

The general shape of the simulated magnitude curves was always a dip in the tested cases. In contrast, the shape of the resonance curve in the phase data varied based on the reader coil configuration. The phase data in Case 1 had a local minimum, or dip, (Fig. 10b). In Case 4, the phase curve had a more complex shape (Fig. 10d). The shape of the curve in the phase data in Case 5 was a peak (Fig. 10f). The baseline of the simulated curves varied based on the reader coil configuration.

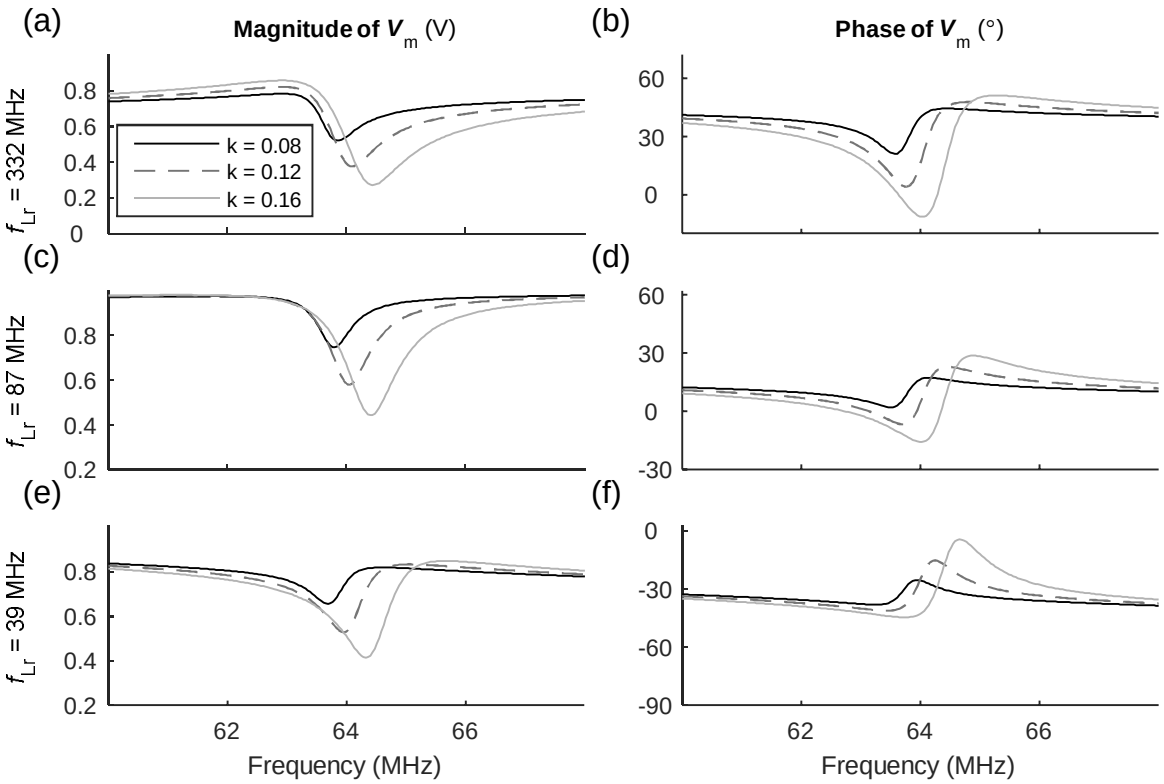

FIGURE10. The simulated magnitude and phase of the complex voltage V_m in three cases where the reader coil configuration was altered. In the first configuration, the self-resonance frequency of the reader coil was much higher than the resonance frequency of the sensor. Next, the self-resonance frequency of the reader coil was slightly higher than the resonance frequency of the sensor. In the last tested configuration, the self-resonance frequency of the reader coil is lower than the resonance frequency of the sensor.

4.3.2 Inductive coupling compensation

The inductive coupling compensation method was studied in [M1] by simulations. The resonance curves were simulated in cases where the reader coil configuration and inductive coupling coefficient were varied. The coil configurations are the same as those presented in Section 4.3.1. The compensation method is based on finding the relation between the height of the resonance curve and the frequency estimate. Here, the compensation method was applied to the data that approximates the measurements of the custom-made reader device and to the data that simulates the measurement of the real part of the impedance by using an impedance analyzer. The frequency estimates (f_{md}, f_{mu} and f_{max}) and the corresponding heights of the resonance curves were extracted from the data. The

scatter plots of these features are given in Fig 11. The relation between the features was approximated using linear regression. In the case of the features f_{md}, or f_{mu}, the relation between the frequency estimates and the heights of the resonance curves is clearly non-linear. Therefore, only the data where the inductive coupling coefficient was from 0.02 to 0.14 was used in the regression modelling. The linear models are also shown in the figures. The first order coefficients of these models (p_1) were used in the compensation method (equation 8). The differences between the compensated frequency estimates and f_0 are given in the figures 11c and 11d. The compensation significantly improved the resonance estimates based on f_{max} compared with the uncompensated estimates [M1]. However, the compensation of the features f_{md}, or f_{mu} only works well when the inductive coupling coefficient is small. In addition, there is always a small difference between f_0 and the compensated estimates in all the tested cases.

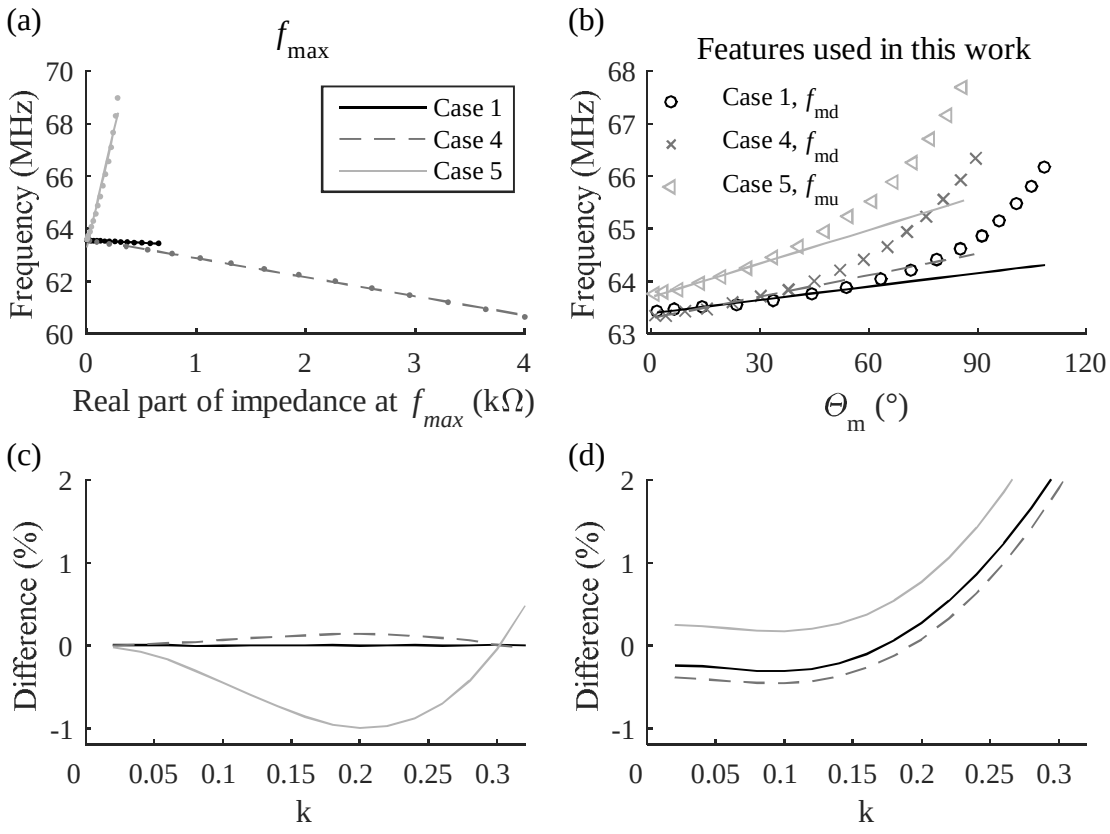

FIGURE 11. The compensation was tested in three cases where the coil configuration and inductive coupling were varied. a) The scatter plot between f_{max} and the real part of impedance at the frequency of f_{max}. b) The scatter plot between f_{md} or f_{mu} and the corresponding Θ_m. c) The difference between compensated f_{max} and f_0 as a function of the coupling coefficient k. d) The difference between the compensated resonance estimates and f_0 as a function of k.

4.3.3 Relation between the extracted features and the sensor parameters

The effects of the sensor capacitance and resistance on the resonance curves and the extracted features were studied in a situation where the reader coil configuration (Case 4) approximated the set-up used in [P4]. In that case, the environment around the sensor influenced both the capacitance (C_s), and the resistance (R_s). Afterwards, the features *FG* and *BWG* were extracted from the measured data. In the physical measurement set-up, there was no sure-fire way to test the method by altering only one parameter at a time, so here the effects of the R_s or C_s on the extracted features are studied with simulations.

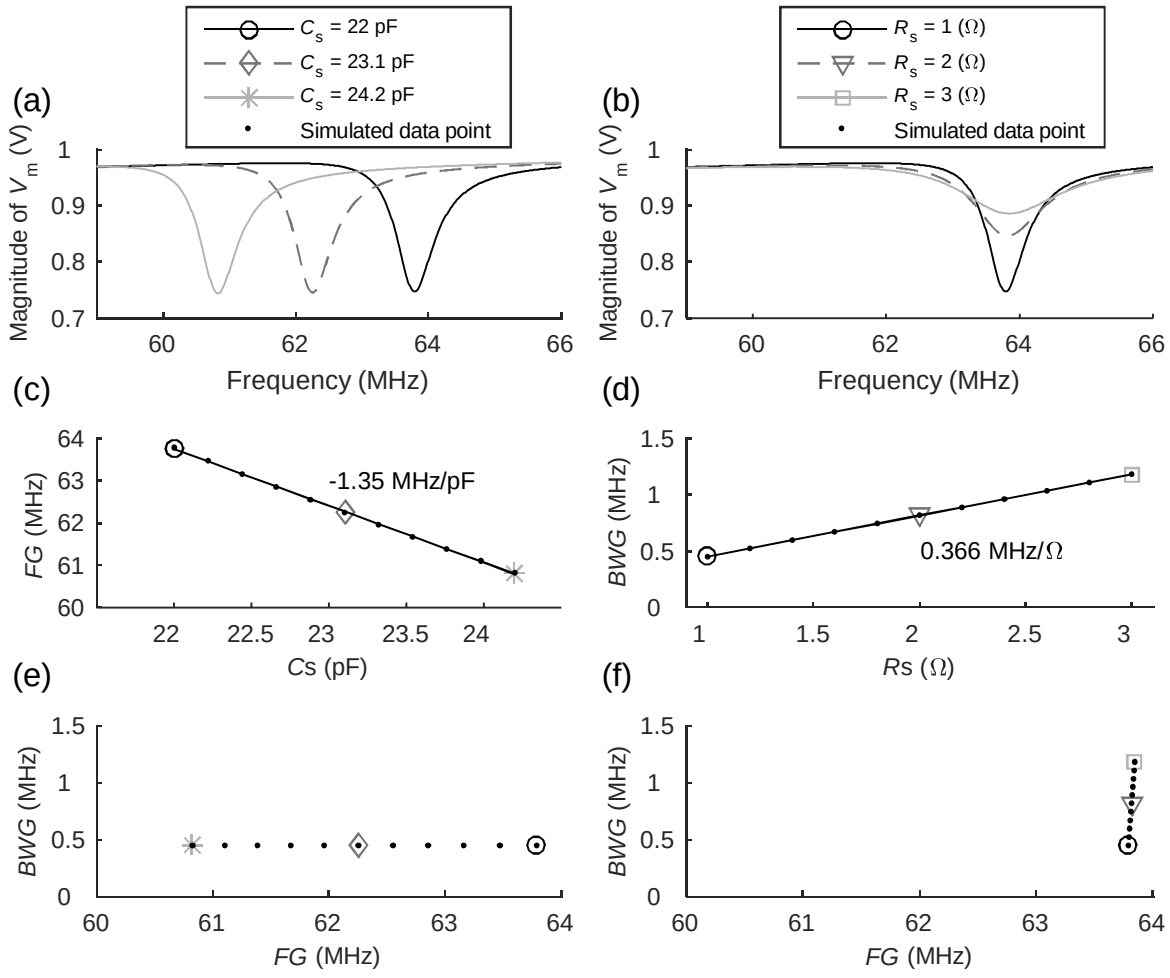

FIGURE 12.a) The effect of the sensor capacitance on the simulated magnitude of V_m. b) The increase in the sensor resistance decreases the depth of the resonance dip. c) The relation between C_s and the resonance frequency estimate *FG*. d) The increase in R_s increases the width of the resonance curve (*BWG*). e) The increase in C_s does not have a significant effect on the feature *BWG*. f) The sensor resistance only has a slight effect on the feature *FG*.

The figures 12a and 12b show the simulated magnitudes of V_m when the capacitance C_s was altered from 22 pF to 24.2 pF, or the resistance, R_s, was changed from 1 Ω to 3 Ω. The changes in C_s altered the resonance estimate *FG* in a fairly linear way in the tested range (Fig. 12c). The effects of the changes in R_s on the width of the resonance curve (*BWG*) are shown in Fig. 12d. In addition, two extracted features (*FG* and *BWG*) are illustrated in scatter plots, where each parameter was altered separately (Figures 12e and 12f). The changes in C_s do not have a significant effect on the feature *BWG, but* the R_s does. However, the increments in the R_s slightly affected the feature *FG* (a 55 kHz increase was noted within the tested range [1 Ω to 3 Ω]).

4.4 Discussion on the simulations

The simulations indicated that the reader coil configuration affects the shape of the resonance curves in the phase data. The simulated and measured resonance curves can be compared in order to analyse the reliability of the simulations. The shapes of the simulated resonance curves in Case 1 resembled the measured phase data shown in Fig 5b. In both cases, the resonance frequency of the reader coil was much higher than the resonance frequency of the sensor and the shape of the resonance curve was a dip. In contrast, the shape of the simulated phase curve in Case 5 is similar to the data measured shown in Fig. 5a where the resonance frequency of the reader coil was smaller than the resonance frequency of the sensor and the shape of the resonance curve was a peak. The magnitude data simulated in Case 4 was similar to the data measured in [P4]. The simulated curves differ from the measured ones because the modelled configurations are not identical with the configurations used in the measurements. In these cases, the similarity was only in the relation between f_{Lr} and f_0. The simplified lumped element model does not fully represent the complexity of physical devices. For example, the baselines of the modelled and measured resonance curves are not the same. The operation of an impedance analyzer was modelled and simulated in [P3] and [M1]. The simulation results were in agreement with the measured verification data. The comparison between the simulated and measured data indicates that the tested model is adequate to predict the shapes of the resonance curves when the reader coil configuration is varied.

The reader coil configuration and the inductive coupling coefficient affect the resonance curves and the accuracy of the resonance estimates, so this was obviously a topic to be studied with the simulations. In the literature, there are two popular readout methods for estimating the resonance frequency. The first method is based on estimating the frequency of the maximum in the real part of the impedance (f_{max}), while in the second method, the frequency of the phase-dip in the impedance

curve (f_p) is estimated. The performance of these two methods, and the methods developed in this thesis have been simulated and discussed in detail in [M1]. Based on the simulated data, the accuracy of the estimate f_{max} was most accurate when the reader coil had the highest self-resonance frequency. In contrast, the accuracy of the phase-dip method was best in the situation (Case 4) where the self-resonance frequency of the reader coil was not as high as possible. The same observation was made in [P3]. The resonance estimates developed in this work (f_{md}, f_{mu} and *FG*) gave acceptable results when the coupling coefficient was small, but their performance became less reliable as the coupling coefficient increased. Moreover, these features had slight differences with $f_{0,}$ even when the coupling was weak.

The inductive coupling compensation method was tested using the simulations explained in Section 4.3.2 and in [M1]. The simulated and the measured features can be compared when the coupling coefficient in the simulation and the measurement distance in the test situation are altered. The behavior of the simulated features (f_{md} and Θ_m) in Case 1 is very similar to the measured data in Fig. 7. In the simulations, the compensation kept the error in the resonance estimate f_c low when the inductive coupling was small (Fig. 11d). However, this effect weakened as the coupling coefficient increased. This is because the relation between f_m and Θ_m is non-linear on a larger scale. In addition, the compensation method was also applied to the resonance estimate f_{max}. The relation between the frequency estimate *(*f_{max}) and the height of the resonance curve was largely linear, and the compensation yielded very good results.

The features *FG* and *BWG* were used to monitor the material around the resonance sensor in [P4], so two features were studied with the simulations. Two parameters, C_s and $R_{s,}$ were altered separately and a scatter plot of the extracted features was drawn up. In these simulations, the *FG* was mainly dependent on the $C_{s,}$ while the *BWG* was mainly dependent on the R_s. According to the data in Fig. 12, the relation between C_s and *FG* and the relation between R_s and *BWG* was almost linear. Thus, the features *FG* and *BWG* are good candidates for monitoring the changes in the equivalent capacitance and the equivalent resistance of the sensor in the tested situation. This helps in developing the methods tested in [P4] because R_s and C_s can be linked to the physical parameters of the environment near the sensor, especially if the methods presented in [26], [33], [44] are used.

The simulation methods developed in this work have greatly increased our understanding of this measurement system. The examples presented here indicate that our simulation methods are well able to predict the actual measurement data. Furthermore, the model can be used to simulate the outputs of several readout methods in the same measurement configuration with an acceptable degree of accuracy, which allows the readout methods to be compared and optimized.

5 Application tests

The readout methods developed here were tested in practical applications that could well benefit from the advantages of measurements based on passive resonance sensors. This chapter describes and discusses the background to the applications, the tested sensors and the results of the experiments. The applications can be divided into two categories: pressure sensing and material monitoring. In the first application, the pressure under compression garments was measured in [P1] and [P2]. The second tested case was the monitoring of the manufacturing process of ceramic slurry. The material was monitored using a sensor installed in the process container [P4]. In the third application, the hydrolysis of a biodegradable material was monitored wirelessly in a buffer solution. In this experiment, simple sensors were encased in the biodegradable materials. These sensors were monitored from outside closed containers as the materials underwent hydrolysis [P5]. Each application had different requirements, which had an effect on the design of the measurement methods. These applications are also interesting measurement problems, per se.

The tested sensors and their operation principles are shortly explained in this chapter. In the compression garment application, the variable capacitors were used to convert the measured pressure into the change of the resonance frequency. This approach is often used in the inductively coupled resonance sensors. However, the electrical fields of inductively coupled passive resonance sensors are not fully confined inside the sensor or its casing, and therefore they interact with their environment. For example, the parasitic capacitances between the coil loops reach beyond their thin sensor casings. The detailed shapes of these parasitic electrical fields are often complicate. A casing or an electrically isolating barrier around the sensor is needed to prevent short-circuits and to diminish the dielectric losses due to the nearby media. The dielectric losses alone can be significant if a large part of the electric field interacts with a conductive material around the sensor, such as a saline solution. Therefore, the interaction between the electric fields and the environment is typically regarded as a source of error. On the other hand, a simple RLC circuit can be used to monitor the environment. This idea was utilized in the material monitoring applications in [P4] and [P5].

5.1 Pressure sensors for compression garments

5.1.1 Introduction to the compression garment application

Compression garments are items of clothing that are supposed to induce a set pressure on the skin. These garments are used, for example, to enhance the healing process of burns and to reduce

swelling in legs [81]. In addition, there are studies to find out if compression garments can be utilized to enhance physical performance [82], balance [83] or recovery after exercise [84]. Although the causes and mechanisms behind the observed effects of these garments are not fully understood, it is clear that the correct pressure is critical for the success of the treatment. While too low a pressure has relatively little effect, too high a pressure may constrict blood circulation and thus cause damage to the tissue. The pressure levels required for compression garments can be very precise, and they vary depending on the standard used [85]. For example, a German RAL standard has four pressure classes ranging from 18 mmHg to 49 and higher [86].

The generated pressure originates from the elasticity of the garment when it is put on. The elasticity and pressure can vary because of the garment's deterioration over time, in addition to which, the shape of the skin and the firmness of the tissue can also play their part. Thus, with such treatments, there is a need to ensure that the correct pressure is always being applied by taking measurements at set points underneath the garment. The pressure can be measured, for example, with commercial pneumatic systems [87]. However, the tubing required for this is difficult to fit under tight clothing, so this measurement method is not only cumbersome, but sometimes it is simply not feasible. A wired capacitive [88] and a piezoresistive [89] sensor have been also tested for this application. In [90] a wearable device was tested for measuring dynamic pressures during running. The aim of the research in this work is to find out whether inductively coupled passive resonance sensors can be used to verify the pressure under these kinds of compression garments, and if so, how accurate would this measurement be.

The two great advantages of inductively coupled passive resonance sensors are that they allow measurements to be taken wirelessly, and with a very simple sensor. Both of these advantages were utilized in the compression garments application. The pressure sensor had to be placed underneath the compression garment, and thus a short-range wireless readout is an ideal solution. In addition, the simple and potentially cheap construction of the sensor could lead to disposable sensors, which would be a great advantage in terms of the hygiene requirements of medical devices. The skin under the compression garment may have sores and wounds, so the same sensor cannot be used for two patients without proper sterilization. Since the sensors may have to be placed all over the body, a feasible hand-held readout device is needed to access the sensors. In this application, the coupling between the reader and the sensor is unknown and can vary, so a means to compensate for the coupling-related errors had to be developed.

5.1.2 The tested pressure sensors

Two different sensor structures were tested for monitoring the pressure under compression garments (Fig. 13). They are both based on RLC circuits, and the sensing property is achieved using pressure-dependent capacitors. A printed circuit board (PCB) is used as a base for the electrical components and the variable capacitors (Fig. 14). The bending element of the capacitors was an elastic Polydimethylsiloxane (PDMS) membrane which deforms under pressure. PDMS, which is of course an electrical insulator, was used because it is biocompatible, in addition to which it is easy to mould into the required shape.

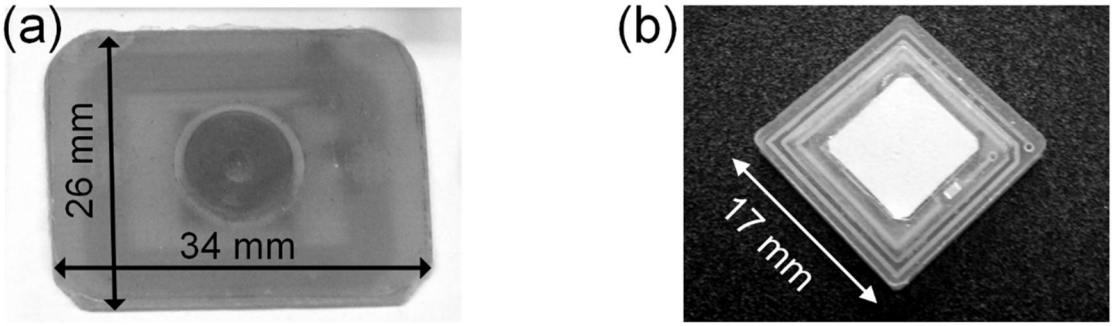

FIGURE 13.Two version of the tested pressure sensors. Both versions have a flexible PDMS-structure and rigid supporting PCB. These layers form a pressure sensitive capacitor.

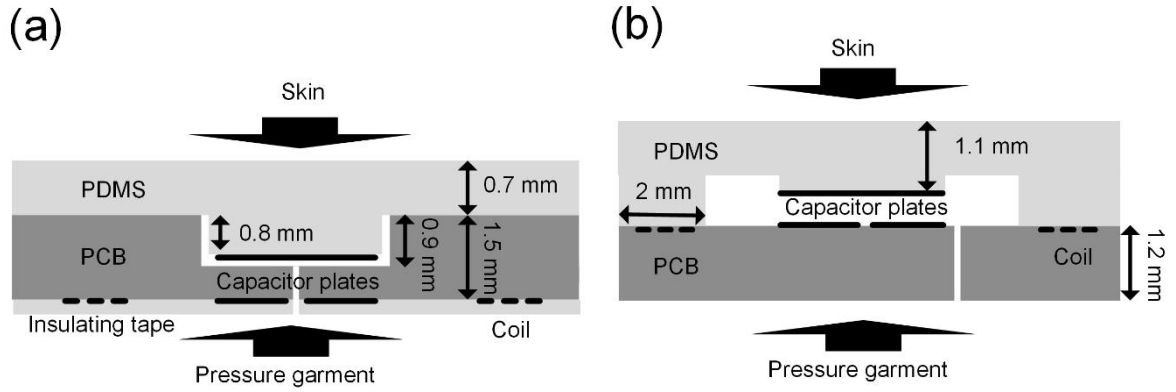

FIGURE 14. a) A schematic drawing of the cross-section of the first design. b) A schematic drawing of the cross-section of the second design.

Both designs had electrically conductive surfaces attached to the deforming structures, which acted as the movable electrodes of the variable capacitors. The structures also had bulk capacitors in parallel with the variable capacitors to adjust the resonance frequencies. An equivalent electrical

circuitry of the first design is presented in [P1]. The static electrodes of the variable capacitors were fabricated on the PCB, and both the sensors had a hole in the PCB that allowed air to escape as the PDMS membrane was deformed.

The structure of the first pressure sensor is shown in Fig. 14a. The aim of this design was to keep the sensor as small and thin as possible; in this case the sensor was 34 mm ´ 26 mm ´ 2.2 mm. To avoid errors arising from the electrical conductivity of the skin or sweat, the metallic parts of the sensor were kept as far away from the skin as possible. In the first prototype, the cavity (diameter 12 mm, height 0.9 mm) that allowed the deformation of the PDMS structure was drilled into the PCB, (Fig. 14a). The second version of the sensor (17 mm ´ 17 mm ´ 3 mm) was designed to be even smaller and more easily fabricated than the first prototype, so it did not have a drilled cavity (Fig. 14b).

5.1.3 Results of the pressure measurements

The basic idea was to measure the relation between the input pressure and the corresponding frequency shift. In the test set-up, a known air pressure was directed onto the PDMS-structure using a rubber film, which modelled the contact with the skin. The air pressure was measured with a Beamex PC105 pressure calibrator. Examples of the measured pressure responses are shown in Fig. 15. More examples of the pressure responses measured with the second design are given in [91] and [P2].

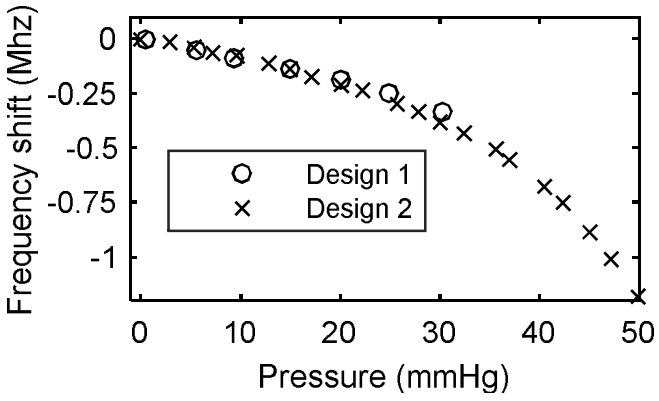

FIGURE 15. Examples of the pressure responses measured with two tested designs.

The first pressure sensor prototype had a sensitivity of −10.7 kHz/mmHg, which had been determined by linear regression [P1]. Because the depth of the cavity in the PCB limited the movement of the membrane, the operation of this sensor was limited to a pressure range of 0 to 30 mmHg. The second prototype had a wider measuring range from 0 mmHg to 50 mmHg. The drawback of the

second design was a non-linear pressure response, which meant that an ANFIS model [92] had to be used to convert the measured frequency shifts into pressure values. The drawback with this method in this application is that the uncertainty in the measurements increased along with any increase in the pressure [91].

In the compression garment application, the inductive coupling between the reader coil and the sensor coil is unknown. When the sensors are measured with the hand-held readout device, the coupling changes along with any change in the distance, angle or alignment between the coils. However, as these changes will, in turn, cause an error in the estimated resonance frequency, a compensation method was used. The usefulness of this method is illustrated in Fig.16. In this test, the readings of the first prototype were measured when the distance of the reader coil from the sensor was changed. The tested garment was designed to create a pressure of over 20 mmHg on the skin. It is clear from the results that the compensation method was able to reduce the error. Based on the data in Fig. 16, without compensation the maximum estimation error would have been roughly 50 mmHg. However, the compensation method only worked well within a limited range. The linear approximation used in the method limits its accuracy in the short measurement ranges. The upper range limit is due to the uncertainty in the extraction of the resonance features from the noisy data when the measurement distance is long. For the first prototype, the valid measurement range was roughly from 1 cm to 4 cm, while for the second prototype, it was from 6 mm to 16 mm.

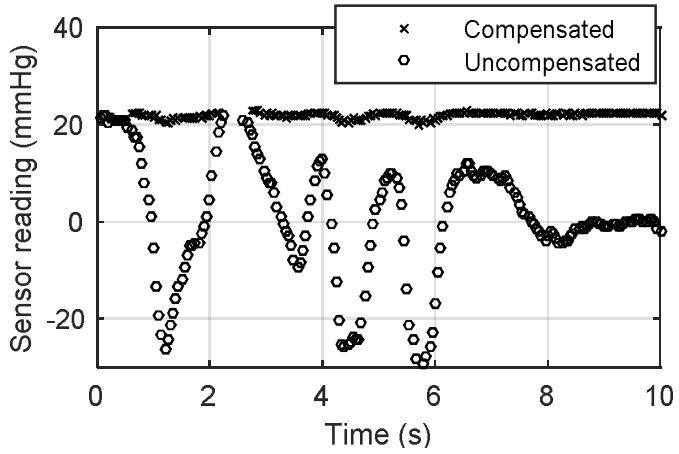

FIGURE 16. The compensated and uncompensated pressure readings measured underneath a compression garment using a resonance sensor and hand-held readout device.

5.1.4 Discussion of the compression garment measurements

Inductively coupled passive resonance sensors were tested in a compression garment application, and it was shown that this short-range wireless readout method could well be better than pressure sensing methods based on air pouches and tubing or wired connection, for a variety of reasons. The tested prototypes had an adequate sensitivity for the application, and although the pressure range of the first design was too narrow, the second design covered the typical pressure range required for compression garments. Thus, the tests show that our pressure sensors do exhibit the required sensitivities and pressure ranges for this kind of application.

There are many ways in which these sensors can be developed further. The mechanical structure of the sensors could be improved in many ways to make them more reliable and easier to mass-produce. The response of the sensor could be made more linear, which would make calibration and error analysis more straightforward. Sensors based on the second design have been studied in [85], [91]. The variation in the pressure responses between the handmade sensors is still problematic and has to be taken into consideration. Because the shape of any sensor disturbs the operation of the compression garments and thus causes measurement errors, the thinner and smoother the shape of the sensor, the fewer the errors. However, this topic has not been studied in more detail due to the lack of a reliable reference method. If a reliable, high-resolution reference method could be developed, then the sensors could be better tested in realistic measurement situations.

In this application, the inductive coupling is unknown, and may vary when the hand-held readout device is used to measure the sensors. In addition, the coil design affects the measurement range, and also the size of the errors caused by the varying inductive coupling. Therefore, compromises have to be made between the measurement distance and the size of the sensor coil. While in the first set-up [P1] neither the reader and sensor coil pair, nor the required cables were optimized to minimize the error caused by the inductive coupling, in the second set-up [P2] a smaller reader coil with a higher self-resonance frequency was used. The inductive coupling still had an effect on the resonance frequency estimates. From this, it seems likely that the combination of both an optimized coil design and a compensation method is needed to reduce the effects of the varying inductive coupling. It must be noted, though, that the measurement distances were longer in the first tested case because larger-diameter coils were used.

The main goal of the measurements was to verify that the compression garment works properly when actually being worn by someone. When the person was stationary, this could be achieved with our hand-held readout device, at least from a distance of a few centimeters. However, there are other issues, such as that capacitive sensing is affected by changes in the sensor's immediate environment. Moisture, for example, can cause significant errors [P2], as can the proximity of skin.

Therefore, in this study the effect of the skin's proximity to the sensor was measured and removed after the sensors had been attached to the skin, as part of the tuning procedure [P1].

Although the tested method has some challenges, such as the size and shape of the sensors and possible problems with moisture, once it has been further developed, the inductively coupled pressure sensors could provide a competitive (and much more feasible) alternative to sensors that require pneumatic tubing or electrical cables.

5.2 Monitoring of particle suspensions

5.2.1 Introduction to suspension monitoring

The continuous monitoring of the quality of suspensions is critical for many current manufacturing processes, including the production of technical ceramics. A ceramic suspension is a combination of particles, water and additives, and there are no existing methods which can adequately fulfill the need for the continuous monitoring of such substances [93]. The typical measurement methods used in this field are rheological measurement [94], centrifugal sedimentation tests [95], and particle size and zeta potential analysis [96]. The main problem with these methods when they are used in industrial applications is the constant need to take samples for laboratory analysis.

An RLC circuit sensor was tested to monitor colloidal suspensions. The tested suspension was aluminum oxide slurry. The composition of a suspension not only has an effect on the resonance frequency of the circuit, but it also affects the losses in the sensor. The tested suspensions contained ions and other components that interact with an electrical field. This causes losses, which were taken into account when designing the signal processing for the measurement system. Some problems can be reduced by the design and encasing of the sensor set-up. For example, the sensor has to be waterproof in order for it to work in a liquid suspension. In addition, these industrial suspensions are often continuously stirred to keep them homogenous, which is also problematic for many measurement probes. However, the short-range wireless link makes it possible to embed the sensor inside the process container while still being able to take continuous measurements as the suspension is being mixed, which is a distinct advantage for this kind of application. Taking samples and transporting them elsewhere for laboratory tests is not a valid option. It is not only labour-intensive, but the quality of the samples deteriorates over time if they are not continuously stirred.

The processing environment of a slurry is very demanding. It is not only full of dust and dirt, but there are strong vibrations and high temperatures which are very problematic for sensitive measurement devices. Such an environment places demands on the readout electronics, which must be tolerant of these demanding conditions. Most impedance analyzers are laboratory devices, and they are not designed to be used in such harsh environments. Therefore, the aims of this study were to design and test a sensor configuration and readout method that can tolerate the environments of suspension and slurry manufacturing processes, and to find out whether the data this measurement method produces can provide useful information that can be utilised to analyze or control such processes.

5.2.2 The methods for suspension monitoring

A system based on inductively coupled passive resonance sensors was built to enable the monitoring of a suspension during a simple, laboratory-scale, aluminium-oxide slurry fabrication process. The resonance sensor was embedded at the bottom of a glass container in which the slurry was processed and stirred continuously. The sensor was measured using the custom-made readout device and placing the reader coil under the container. The folded structure of the sensor is thin, durable and it was ensconced at the bottom of the container under a layer of epoxy resin. A diagram of a cross-section of the sensor set-up and a picture of the embedded sensor are shown in Fig. 17. The thickness of the epoxy layer is used to control the sensitivity of the sensor and can thus limit the effect of the losses due to the conductivity of the slurry. Without the epoxy layer, the excessive losses would dissipate the resonance curve to an undetectable level. Two features were extracted from the measured data: the frequency (*FG*) and width (*BWG*) of the dip in the gain curve (Fig. 6f). These features were selected because they can both be extracted from the same measured curve. The changes of *FG* were linked to the changes in the real part of the relative permittivity of the measured medium. The changes in the *BWG* were linked to the changes in the imaginary part of the relative permittivity, and to the changes of other losses in the system.

The tested slurry contained three components: water, aluminium oxide particles and a dispersing agent. The components were added incrementally, and mixed into the suspension. In the first part of the process, the dispersing agent was added to water. Then, aluminium oxide was mixed into the suspension in small batches. The response curves were measured after each increment, once the added material had been fully mixed. The same process was repeated, and before the actual measurements were taken, a sample of isopropanol was measured to check if the response of the monitoring system to a known liquid remained consistent. A more detailed description of the slurry fabrication, measurement set-up, signal processing, and more results, can be found in [P4].

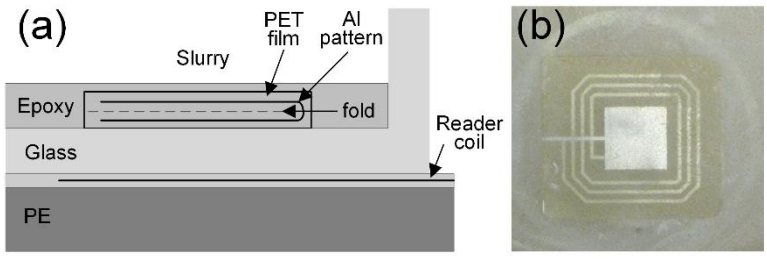

FIGURE 17. a) A diagram of the cross-section of the folded sensor structure. b) A picture of the sensor embedded in epoxy at the bottom of a container.

5.2.3 Results of the slurry monitoring test

The estimate for the resonance frequency *FG* was found to be a good indicator for the added dispersing agent and aluminium particles because of the nearly linear responses (Fig. 18). It should be noted that the aluminium oxide alone is not soluble in water and cannot be mixed in water in large quantities without a dispersing agent. Thus, the measured response is characteristic of this suspension, but not of a pure mix of aluminium oxide and water. Each added increment of the dispersing agent decreases the *FG* and each increment of aluminium oxide increases the *FG*. When measuring the shift due to the dispersing agent, the initial values for *FG* in water were 76.78 MHz and 76.76 MHz for series 1 and series 2, respectively. When measuring the aluminium oxide, the shift was calculated by comparing the *FGs* with the point at which all the dispersing agent had been added to the water. The values of *FG* at these points were 76.22 MHz and 76.16 MHz for series 1 and series 2, respectively.

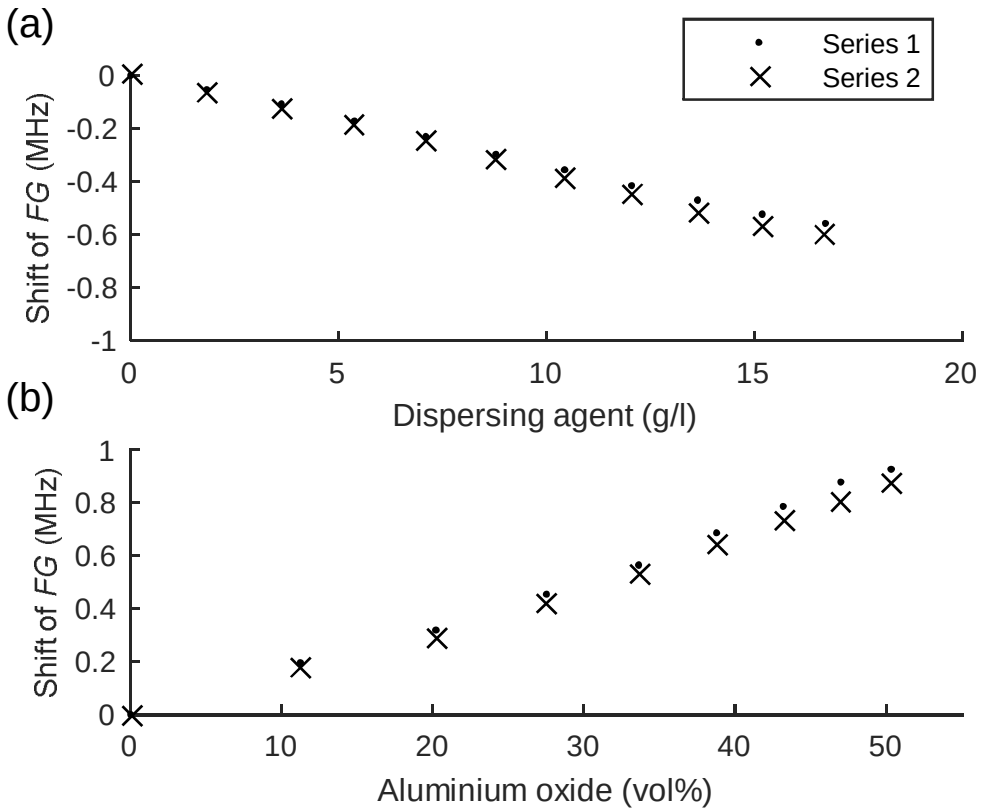

FIGURE 18. a) The resonance frequency estimate *FG* decreases as dispersing agent is added. b) The feature *FG* increases as the aluminium oxide is added to the suspension.

The state of a complex suspension cannot be adequately explained with one single feature, so a more complex analysis was needed. A scatter plot was made using the features *FG* and *BWG*, as shown in Fig. 19. These features were calculated from the same two experiments discussed above. The data points in the scatter plot illustrate the state of the two monitored fabrication processes. The results are similar, although not exactly the same. The actual process was started by pouring deionized water into the container. Next, the diluted dispersing agent was added to the solution. Each increment is clearly detectable. Once all the dispersing agent had been mixed into the solution, the aluminum oxide was added in small increments in order to create the suspension. There was a distinct difference between the two series of measurements, especially when the aluminum oxide was added.

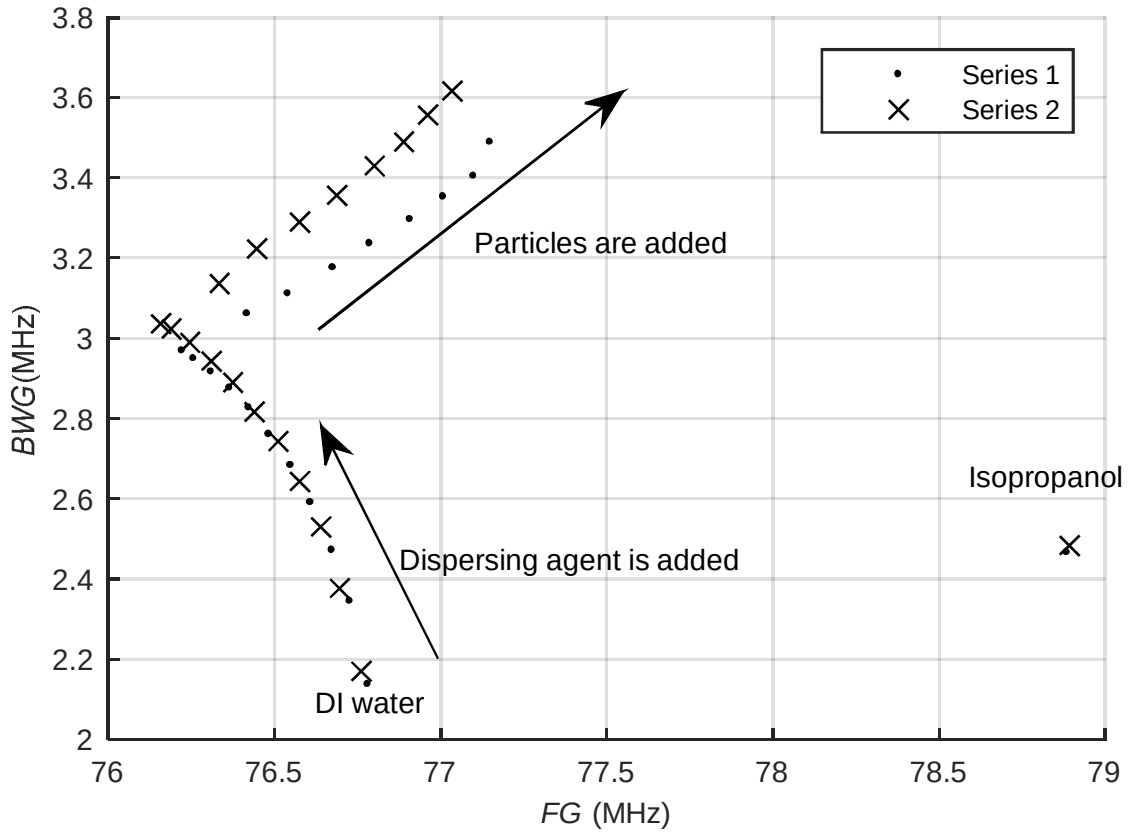

FIGURE 19. A scatter plot of the extracted features was made to illustrate the two monitored aluminium oxide fabrication processes. The data points illustrate the states of the processes where a portion of either dispersing agent or aluminium oxide was added and mixed into the suspension. The isopropanol was measured as a reference before each process.

5.2.4 Discussion of the suspension monitoring

There are a number of manufacturing processes which could benefit from continuous measurements and monitoring, but it is a challenge to develop and introduce reliable and easy-to-use measurement systems for industrial applications. The monitoring method presented here is simple and robust, and thus has great potential as an on-line monitoring system. The extracted features can be linked to the constituents of the suspension, and the results showed that the different states of the suspension manufacturing processes tested here can be monitored.

There was a discernible difference between the two tested processes. The most likely reasons for this are the dosage of the added ingredients and the mixing process of the aluminum oxide, as the reference measurement with isopropanol only showed a very slight difference. At this stage of its development, the repeatability of the measurement system and the discernible differences in the measurement results when the suspension was altered can be regarded as a good starting point. It seems more than likely that this method can be used to detect differences in similar sequential fabrication processes. This would mean that problematic intermediate steps in the process can be monitored and, hopefully, corrected before they alter the final product, when it is too late to react.

Obviously, the two features extracted in these experiments cannot completely capture the chemical and physical complexity of any suspension. The links between these features and the state of the suspensions in the process need further study. This would entail linking the chemistry and the physical phenomena in the suspension to its permittivity. In theory, the state of the suspension could even be expressed as a change of the components in the RLC resonator model. However, this link in the measuring chain would have to be specific to each type of suspension, and to one sensor structure. It is clear that modelling the link between the suspension and RLC circuit is important, but this is a complex task which is beyond the scope of this research.

Another problem is that the measurement method presented here is sensitive to the temperature, and is thus much better suited to processes which use a regulated temperature. In addition, any unknown impurities in the solution, like salts, will also affect the state of the suspension and thus make the analysis more complex. Each suspension process will have its own individual effect on the extracted features, so the method has to be verified separately for each process.

5.3 Monitoring of biodegradable polymers in vitro

5.3.1 Introduction to the monitoring of biodegradable polymers

Small yet robust inductively coupled passive resonance sensors were tested to monitor the properties of biodegradable materials. The sensors can be embedded directly into the materials under test, and wireless measurements can be taken from a distance of a few centimeters. Thus, the material can be placed in a sealed container where its environment can be controlled. The biodegradable materials studied here are used as orthopedic implants and scaffolds in tissue engineering. One of the challenges of working with these materials is that their degradation rate can vary according to their environment [97], yet such biodegradable materials have to maintain their properties for a predetermined time. Thus, medical biodegradable materials are extensively tested *in vitro* before they are put to their intended use. In an ideal world, the implants would be monitored *in vivo,* since the degradation process may differ from person to person [97], but this is rarely practical. The *in vitro* testing of biodegradable materials is typically done by taking samples at set intervals and analyzing them later in a laboratory. Typical testing methods include mechanical testing and weighing dried samples to measure their water absorption. In addition, measurements of viscosity and differential scanning calorimetry are also used to characterize biodegradable polymers in hydrolysis. Most of these methods either consume or alter the tested sample, so the monitoring cannot be continuous [98]. In this research, one of the goals was to see whether biodegradable polymers can be monitored using inductively coupled passive resonance sensors, and to find out whether these measurements match up to the results from existing methods.

5.3.2 Methods for monitoring polymers during hydrolysis

The wireless monitoring set-up that was used to test biodegradable polymers is shown in Fig. 20a. This set-up was based on the initial experiments presented in [99]. The resonance sensor circuits were made using a 4-layer printed circuit board process. Hence, the sensors do not have any external components or soldered joints, as seen in Fig. 20d. This approach was taken in order to enable the sensor to withstand the encapsulation process. Interdigital capacitors were used to monitor the polymer as seen in the figures 20c and 20d.

The resonance circuits were embedded in the polymers (Fig. 20b). The encapsulation process is described in [100]. The tested polymers were Poly(L-lactide-co-glycolide) (PLGA 80/20) and poly-DL-lactide-co-glycolide) (PDLGA 85/15). These polymers are similar chemically, but have different degradation rates. Next, the samples were placed in a Sörensen buffer solution kept at 37 °C. The

resonance circuits were measured using a reader coil placed under the container. The custom-made readout device was used to measure the reader coil and the embedded resonance circuit.

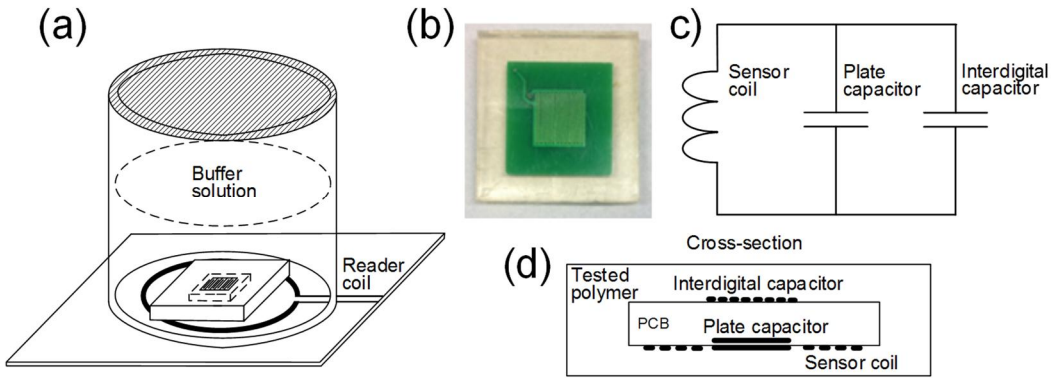

FIGURE 20. a) The measurement set-up. b) The sensor embedded in in the tested polymer. c) A schematic of the sensor circuit. d) The drawing of the cross-section of the embedded sensor.

5.3.3 Results of the polymer degradation tests

Five samples for each tested material (PLGA 80/20 and PDLGA 85/15) and the reference series for conventional measurements were prepared. According to the reference test results, PLGA 80/20 degraded only slightly within 60 days, whereas over the same period, the PDLGA 85/15 decayed to such a degree that it lost its mechanical properties. The results of the reference measurement methods can be found in [P5] and in more detail in [100]. The change of the estimated frequency of the minimum in the measured phase curve f_{md} is shown in Fig. 21a. The changes were calculated by comparing the extracted features with the situation just after immersion in a buffer solution. Both materials had rather monotonic signals after a short drop during the first days in hydrolysis. The feature f_{md} of the circuits in PDLGA started to decrease significantly after approximately six weeks. The change in the estimated width of the measured phase curve BW_p is illustrated in Fig. 21b. Here, the signal from PDLGA 85/15 is not monotonic but has three different phases. Interestingly, the changes in BW_p did not occur simultaneously with the changes of the f_{md}.

Although the shape of the circuit eased the encapsulation process, a significant increase in the feature BW_p between adjacent data points indicated that four of the encapsulations (two samples of each material) had failed, at least partially, during the encapsulation. This phenomenon was more easily detectable from the samples in PLGA 80/20. Despite the partial failure, the measurement signals from the circuits were still detectable in many cases, although they cannot be fully relied upon to represent the degradation of the tested material. The compromised signals are represented by the light gray color in Fig. 21.

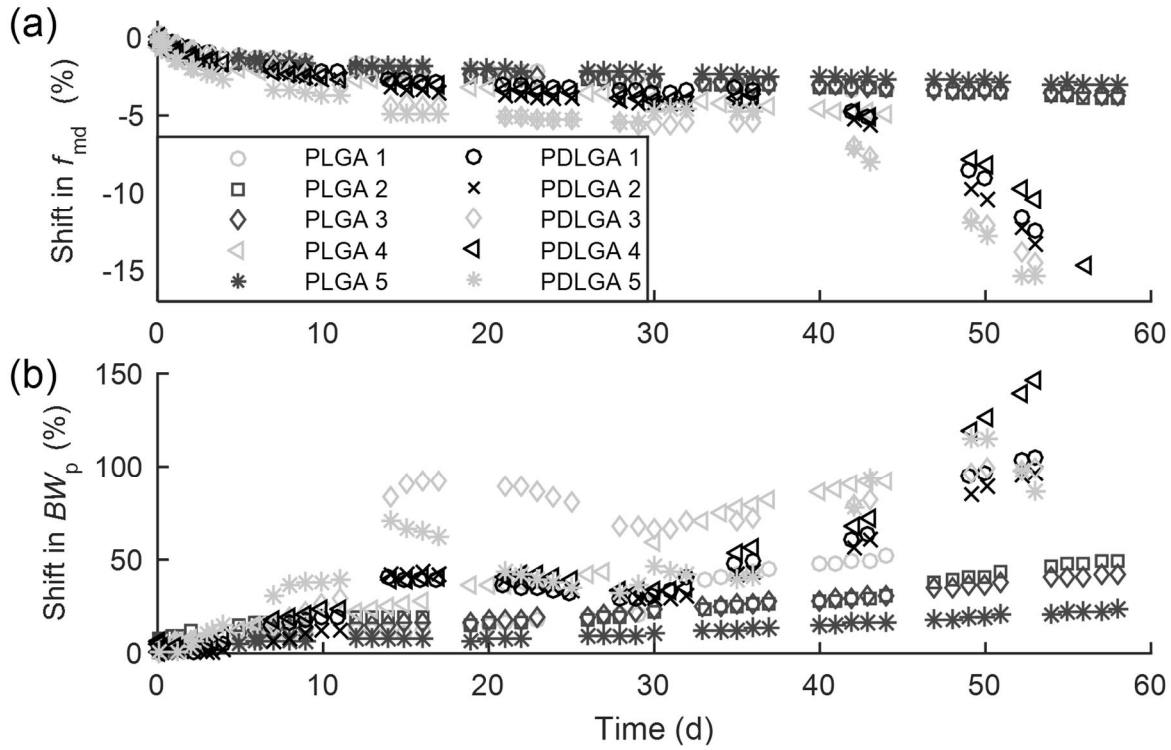

FIGURE 21. a) The estimated frequency of the minimum in the measured phase curve (f_{md}) indicates the initial water absorption and possibly the degradation process of PDLGA after 6 weeks in hydrolysis. b) The estimated width of the measured phase curve (BW_p) of PLDGA samples had multiphase behavior. The samples in PDGA had monotonic responses with this timescale.

5.3.4 Discussion on polymer degradation monitoring

A novel method for monitoring biodegradable polymers *in vitro* was tested. The method yields two features (f_{md} and BW_p) that change as the hydrolysis proceeds. The shifts of these features are typical for each tested polymer. The hydrolysis series indicated that the method may provide data that cannot be easily captured by conventional measurement methods, which are typically based on sampling. Our method was generally able to distinguish the changes that occurred within a day, which shows as a steady drift in the measured signals. Conventional monitoring methods yield much sparser data.

Based on the reference measurements [100], the PLGA 80/20 material did not degrade significantly during hydrolysis within 60 days. There was only a slight decline in the measured viscosity [P5], and although the inductively measured signals showed a detectable drift, there were no major changes (Fig. 21). In contrast, the signals from the PDLGA 85/15 samples had significant changes, in addition

to which, neither of the two signals (f_{md} and BW_p) changed at the same time. The data in Fig. 21b indicates that the hydrolysis of PLGA 85/15 has several phases. The drop in the feature f_{md} coincided with the drop in class transition temperature [P5]. The sampling frequency of the reference monitoring methods in this test series was inadequate for a more detailed analysis. The presented monitoring method may become useful if, for example, the effect of the environment on the rate of hydrolysis is studied. The environment of the encapsulated polymer can be varied, and the changes in the features could be monitored continuously online.

This monitoring method may also be useful for biodegradable implants. A sensor made of biodegradable materials could predict the premature failure of the implants. However, such applications are extremely demanding and may require significant investment in research and development before practical commercial devices can be produced. Future biodegradable implants may well be based on the technologies tested in [32], [37], [101]–[103]. According to the data measured in [P5], the modulus of the PDLGA declined throughout the experiment, but this data was so sparse that it was impossible to determine if the mechanical state of the polymer can be detected from the inductively measured features. Linking the measured features to the changes in the polymers is still an open question and requires further research.

The monitoring method presented here still needs improvements. In order to encapsulate the test circuits, there has to be a reliable way to process the material to be tested. This may be a problem with newer, more interesting materials, since typically there is a limited amount of the material available and the processing parameters have to be experimented with. In addition, our tests showed that the encapsulation around the circuits is prone to cracking. This causes the features to shift unexpectedly, which makes them more complex to interpret, and therefore less reliable. The extracted features are also prone to changes in the test environment, such as the temperature and the conductivity of the hydrolysis solution.

6 Conclusions

The objective of this research was to study a measurement method based on inductively coupled resonance sensors. This method has two distinct advantages over other measurement methods. It not only provides a way to take short-range wireless measurements, but the construction of the sensor itself is very simple. The measurement distance is, by and large, limited to the dimensions of the coils in the inductive link. The inductive coupling can be optimized, but the measurement distance remains a very limiting factor. This means that our method is not a general-purpose wireless measurement method, as most radio-based systems have longer communication distances. However, our method provides an easy way to take measurements in applications where the measurement target is just underneath the surface of a material. The inductive coupling allows the signals to be transmitted through thin materials without compromising the structural integrity of the material by using wires or cables. One obvious constraint with this method is that the magnetic field of the inductive link does not penetrate metallic materials. Nevertheless, by utilizing an analog inductive link, the sensor does not require connectors, cables, semiconductor components or power management circuits. This simplicity makes the method favorable in applications where the sensor has to be disposable, and thus cheap to manufacture. In addition, the robust structure of the sensor can withstand harsh environments.

Recent developments in instrumentation, materials and signal processing have prompted a review of measurement methods based on inductively coupled passive resonance sensors. The importance of the sensor element for the overall performance of a measurement system is obvious. There are many sensing elements whose resistance, inductance or capacitance is altered by the measurand, and so they can be used in inductively coupled sensors. These elements are very similar to the ones used in conventional measurement systems, so their performance is not the main limiting factor. Therefore, the limitations of these methods are likely to exist elsewhere in the measurement chain. The performance of the readout device and the signal processing methods may have a significant effect on the feasibility, versatility and reliability of an inductively coupled measurement system. Therefore, the readout methods for inductively coupled passive resonance sensors were analyzed and developed in this thesis, as shown in the included publications. In addition, the functionality of the methods was evaluated by simulations. The developed readout methods were also applied to three practical measurement problems.

The first research question was: *What kind of readout methods are needed to increase the feasibility and versatility of inductively coupled passive resonance sensors?*

This question was answered by specifying and producing a custom-made readout device and by developing the signal processing. The developed methods were then tested and improved in various applications. The readout method of the custom-made device is simpler than the method which measures true impedance. The custom-made reader device can make repeated fast frequency sweeps. The impedances of the reader coils and the resonance sensors modify the gain and phase curves, which are measured against a reference channel. The implementation of the readout electronics is straightforward and compact. The advantage of using a custom-made readout device is that the measurement system can be more easily configured and modified to suit the requirements of the application. Being able to access raw measurement data is an advantage for signal processing development, as the use of current commercial measurement devices is restricted by technical specifications and data types which have already been determined by the original designer. The main drawback with custom-made devices is the difficulty of reproducing the experiments elsewhere, because not all research groups have access to the similar devices.

Methods were developed to process the measurement data from the custom-made readout device. The core principles of the signal processing are presented in [P1], where the method was successfully used to estimate the resonance frequency of an inductively coupled RLC circuit. The signal processing methods were later modified in order to account for the losses in the resonance circuit, in [P4, P5]. The shape and the position of the measured resonance curves can vary significantly in the tested applications, but our methods were found to be robust and easily adjustable. A key feature of the developed methods is the interpolation of the resonance characteristics from discrete data using polynomial regression. This method does not require detailed information about the components in the measurement system. The tested readout methods are a compromise between simplicity, performance and accuracy, and have yet to be further optimized.

The second research question was: "*How do the properties of the reader coil and the variations in inductive coupling affect the measured resonance curves and the extracted features?*"

The effects of the coil configuration and inductive coupling on the resonance curves were simulated and examined in [P3] and [M1], as well as in Chapter 4 of this thesis using a lumped element model. The basic functionality of the simulation was verified by the measurements. In addition, the simulation was able to predict the shape of the measured curves when the inductive coupling was varied.

The simulation allowed the methods developed in this work to be compared with those methods presented in the literature in the same measurement configuration.

Based on the simulations, there was no single method that would have been the best in all the test cases. The readout methods based on measuring the frequency of the local maximum in the real part of the impedance and the frequency of the phase dip worked well when the reader coil configuration had been set to favor those methods. In a real measurement situation, however, these conditions cannot always be achieved. In addition, these methods worked fine when the inductive coupling coefficient was very small. All the tested methods worked fine in situations where the inductive coupling was kept constant and the sensor capacitance was varied to simulate changes in the measur- and [M1]. The performance of the readout methods presented in this thesis was fairly similar regardless of the reader coil configuration. Three of the configurations used in [M1] are similar to the measurement set-ups used in [P1], [P2] and [P4] and the simulation results were in agreement with the results measured in the publications. The lumped element model and the simulation methods provide a useful tool for testing and optimizing the signal processing in known measurement configurations. Furthermore, simulations can be used to optimize the measurement configuration and thus help avoid errors and ambiguities in the resonance estimates.

The third research question was: *Can the effects of an unknown inductive coupling on the estimates for the resonance frequency be compensated for?*

The variations in the inductive coupling can cause significant errors in the estimates of the resonance frequency. The influence of this phenomenon can be mitigated by measuring the height of the resonance curve and using it to compensate for the error. This principle was utilized in the compensation algorithm that was introduced in [P1] and further studied and tested in [P2]. The method was able to reduce the effects that the variations in inductive coupling had on the resonance frequency estimates. The compensation was valid within a certain range of inductive coupling coefficients, but problems arose when the measurement distance was very short. The simulations were used to test the compensation scheme in [M1], and these simulations indicated similar behavior to what had already been detected in the measurements in [P1, P2]. The compensation method was also applied to one of the readout methods presented in the literature. The compensation method gave very good results when it was applied to resonance estimates that are based on the measurement of the real part of the impedance.

The developed readout methods were designed to test inductively coupled passive resonance sensors in new applications. These applications were selected in order to demonstrate the potential benefits of the measurement method. In the first case, the pressure underneath a thin compression garment was measured [P1, P2]. For hygienic reasons, this application would benefit from the use

of cheap, simple disposable sensors. This application also required compensation for the inductive coupling, because the measurement distance is bound to vary when using a hand-held readout device. The compensation method kept the errors in the resonance estimates relatively small in comparison with the sensitivity and accuracy that a capacitive sensor needs for this application, so it can be stated that the performance of our measurement method was acceptable for this application. However, the sensor part would have to be redesigned to improve its mechanical durability and to make it suitable for mass production before one can achieve the benefits of the original idea of using disposable sensors.

The robustness of the sensor part was utilized in two applications where the sensor was encapsulated into a material in order to detect changes in the permittivity of its environment. In the particle suspension application, the sensor was installed into a container in which a fabricated slurry was being constantly mixed [P4], so the measurements were taken during the mixing. Initial testing indicated that the method was sufficiently sensitive to monitor the composition of the slurry well enough to be able to utilize the measurements for, say, control feedback for the manufacturing process. So there is a proof of concept that the developed methods can be used for monitoring liquid suspensions in industry, but further testing with a large number of different suspensions is needed to fully determine the usefulness and limitations of the method.

Small wirelessly measured bio-stable sensors were encapsulated in different biodegradable polymers. The encapsulated sensors were monitored during hydrolysis to find out if changes in the polymers could be detected. The measurement of biodegradation is important, because this process is known to vary *in vivo,* so the safe use of biodegradable implants requires highly controlled degradation. A monotonic drift was observed in the measured resonance signals, which indicates that this method may provide a means for more continuous monitoring of biodegradable implants if the link between the measured changes and the biodegradation changes in the polymer can be confirmed. The method was also able to detect a difference between two similar polymers that had different degradation profiles. However, the relationship between the measured features and the physical and chemical parameters of the polymer during the hydrolysis still require further study. In addition, in order to monitor biodegradable implants, this measurement method needs biodegradable sensors that remain stable longer than the lifetime of the implant.

Further development of this measurement method and its use in different application domains requires multidisciplinary optimization and problem solving. There are many ways to implement readout devices, and this thesis has only investigated a few of them. New signal processing options can be developed and optimized using modelling. For example, optimizing the feature extraction in cases where the number of measured data points are minimal and noise is included in the model

could make the measurements faster. Perhaps one of the most interesting aspects for any researcher developing these kinds of systems is to identify which part of the measurement chain creates problems, and how they can easily be solved.

References

[1] M. M. Rodgers, V. M. Pai, and R. S. Conroy, “Recent Advances in Wearable Sensors for Health Monitoring,” *IEEE Sens. J.*, vol. 15, no. 6, pp. 3119–3126, 2015.

[2] S. C. Mukhopadhyay, “Wearable Sensors for Human Activity Monitoring: A Review,” *IEEE Sens. J.*, vol. 15, no. 3, pp. 1321–1330, 2015.

[3] A. Deivasigamani, A. Daliri, C. H. Wang, and S. John, “A Review of Passive Wireless Sensors for Structural Health Monitoring,” *Mod. Appl. Sci.*, vol. 7, no. 2, pp. 57–76, Jan. 2013.

[4] Aqeel-ur-Rehman, A. Z. Abbasi, N. Islam, and Z. A. Shaikh, “A review of wireless sensors and networks’ applications in agriculture,” *Comput. Stand. Interfaces*, vol. 36, no. 2, pp. 263–270, Feb. 2014.

[5] T. Ojha, S. Misra, and N. S. Raghuwanshi, “Wireless sensor networks for agriculture: The state-of-the-art in practice and future challenges,” *Comput. Electron. Agric.*, vol. 118, pp. 66–84, 2015.

[6] M. Amiribesheli, A. Benmansour, and A. Bouchachia, “A review of smart homes in healthcare,” *J. Ambient Intell. Humaniz. Comput.*, vol. 6, no. 4, pp. 495–517, 2015.

[7] J. Yick, B. Mukherjee, and D. Ghosal, “Wireless sensor network survey,” *Comput. Networks*, vol. 52, no. 12, pp. 2292–2330, 2008.

[8] I. F. Akyildiz, W. Su, Y. Sankarasubramaniam, and E. Cayirci, “Wireless sensor networks: a survey,” *Comput. Networks*, vol. 38, no. 4, pp. 393–422, Mar. 2002.

[9] J. Gubbi, R. Buyya, S. Marusic, and M. Palaniswami, “Internet of Things (IoT): A vision, architectural elements, and future directions,” *Futur. Gener. Comput. Syst.*, vol. 29, no. 7, pp. 1645–1660, 2013.

[10] J. Fernández-Salmerón, A. Rivadeneyra, F. Martínez-Martí, L. F. Capitán-Vallvey, A. J. Palma, and M. A. Carvajal, “Passive UHF RFID tag with multiple sensing capabilities,” *Sensors*, vol. 15, no. 10, pp. 26769–26782, 2015.

[11] C. C. Collins, “Miniature passive pressure transensor for implanting in the eye,” *IEEE Trans. Biomed. Eng.*, vol. 14, no. 2, pp. 74–83, 1967.

[12] R. S. Mackay and B. Jacobson, “Endoradiosonde,” *Nature*, vol. 179, no. 4572, pp. 1239–1240, Jun. 1957.

[13] Q.-A. Huang, L. Dong, and L.-F. Wang, “LC Passive Wireless Sensors Toward a Wireless Sensing Platform: Status, Prospects, and Challenges,” *J. Microelectromechanical Syst.*, vol. 25, no. 5, pp. 822–841, Oct. 2016.

[14] Joint Committee for Guides in Metrology, “International vocabulary of metrology - Basic and general concepts and associated terms (VIM),” 2012. [Online]. Available: https://www.bipm.org/utils/common/documents/jcgm/JCGM_200_2012.pdf

[15] K. Finkenzeller, *RFID Handbook: Fundamentals and Applications in Contactless Smart Cards, Radio Frequency Identification and near-Field Communication*, 3rd ed. Wiltshire: John Wiley & Sons, Ltd, 2010.

[16] P. Rawat, K. D. Singh, H. Chaouchi, and J. M. Bonnin, “Wireless sensor networks: a survey on recent developments and potential synergies,” *J. Supercomput.*, vol. 68, no. 1, pp. 1–48, Apr. 2014.

[17] T. Rault, A. Bouabdallah, and Y. Challal, “Energy efficiency in wireless sensor networks: A top-down survey,” *Comput. Networks*, vol. 67, pp. 104–122, 2014.

[18] J. Riistama, J. Väisänen, S. Heinisuo, H. Harjunpää, S. Arra, K. Kokko, M. Mäntylä, J. Kaihilahti, P. Heino, M. Kellomäki, O. Vainio, J. Vanhala, J. Lekkala, and J. Hyttinen, “Wireless and inductively powered implant for measuring electrocardiogram,” *Med. Biol. Eng. Comput.*, vol. 45, no. 12, pp. 1163–1174, Nov. 2007.

[19] M. Ghovanloo and S. Atluri, “A Wide-Band Power-Efficient Inductive Wireless Link for Implantable Microelectronic Devices Using Multiple Carriers,” *IEEE Trans. Circuits Syst.*, vol. 54, no. 10, pp. 2211–2221, Oct. 2007.

[20] J. Zhang, G. Tian, A. Marindra, A. Sunny, and A. Zhao, “A Review of Passive RFID Tag Antenna-Based Sensors and Systems for Structural Health Monitoring Applications,” *Sensors*, vol. 17, no. 2, p. 265, 2017.

[21] B. S. Cook, R. Vyas, S. Kim, T. Thai, T. Le, A. Traille, H. Aubert, and M. M. Tentzeris, “RFID-Based Sensors for Zero-Power Autonomous Wireless Sensor Networks,” *IEEE Sens. J.*, vol. 14, no. 8, pp. 2419–2431, Aug. 2014.

[22] C. Occhiuzzi, S. Caizzone, and G. Marrocco, “Passive UHF RFID Antennas for Sensing Applications: Principles, Methods, and Classifications,” *IEEE Antennas Propag. Mag.*, vol. 55, no. 6, pp. 14–34, 2013.

[23] V. Viikari, H. Seppä, and D.-W. Kim, “Intermodulation Read-Out Principle for Passive Wireless Sensors,” *IEEE Trans. Microw. Theory Tech.*, vol. 59, no. 4, pp. 1025–1031, Apr. 2011.

[24] V. Viikari, J. Song, and H. Seppä, “Passive Wireless Sensor Platform Utilizing a Mechanical Resonator,” *IEEE Sens. J.*, vol. 13, no. 4, pp. 1180–1186, Apr. 2013.

[25] R. A. Potyrailo, H. Mouquin, and W. G. Morris, “Position-independent chemical quantitation with passive 13.56-MHz radio frequency identification (RFID) sensors,” *Talanta*, vol. 75, no. 3, pp. 624–628, May 2008.

[26] K. G. Ong, C. A. Grimes, C. L. Robbins, and R. S. Singh, “Design and application of a wireless, passive, resonant-circuit environmental monitoring sensor,” *Sensors Actuators A Phys.*, vol. 93, no. 1, pp. 33–43, Aug. 2001.

[27] F. E. Terman, R. A. Helliwell, J. M. Pettit, D. A. Watkins, and W. R. Rambo, *Electronic and radio engineering*, 4th ed. McGraw Hill, 1955.

[28] P.-J. Chen, S. Saati, R. Varma, M. S. Humayun, and Y.-C. Tai, “Wireless Intraocular Pressure Sensing Using Microfabricated Minimally Invasive Flexible-Coiled LC Sensor Implant,” *J. Microelectromechanical Syst.*, vol. 19, no. 4, pp. 721–734, Aug. 2010.

[29] J. Coosemans, M. Catrysse, and R. Puers, “A readout circuit for an intra-ocular pressure sensor,” *Sensors Actuators A Phys.*, vol. 110, pp. 432–438, 2004.

[30] S. S. Mohan, M. del Mar Hershenson, S. P. Boyd, and T. H. Lee, “Simple accurate expressions for planar spiral inductances,” *IEEE J. Solid-State Circuits*, vol. 34, no. 10, pp. 1419–1424, 1999.

[31] M. A. Fonseca, J. M. English, M. von Arx, and M. G. Allen, “Wireless micromachined ceramic pressure sensor for high-temperature applications,” *J. Microelectromechanical Syst.*, vol. 11, no. 4, pp. 337–343, Aug. 2002.

[32] M. Luo, A. W. Martinez, C. Song, F. Herrault, and M. G. Allen, “A Microfabricated Wireless RF Pressure Sensor Made Completely of Biodegradable Materials,” *J. Microelectromechanical Syst.*, vol. 23, no. 1, pp. 4–13, Feb. 2014.

[33] S. Zhang, “Passive inductively coupled wireless sensor for dielectric constant sensing,” Doctoral dissertation, The University of Texas at Austin, 2013.

[34] M. Maksimović, G. M. Stojanović, M. Radovanović, M. Malešev, V. Radonjanin, G. Radosavljević, and W. Smetana, “Application of a LTCC sensor for measuring moisture content of building materials,” *Constr. Build. Mater.*, vol. 26, no. 1, pp. 327–333, Jan. 2012.

[35] V. Sridhar and K. Takahata, “A hydrogel-based wireless sensor using micromachined variable inductors with folded flex-circuit structures for biomedical applications,” in *2008 IEEE 21st International Conference on Micro Electro Mechanical Systems*, 2008, pp. 70–73.

[36] C. M. Boutry, H. Chandrahalim, and C. Hierold, “Characterization of RF Resonators Made of Biodegradable Materials for Biosensing Applications,” *Procedia Eng.*, vol. 25, pp. 1529–1532, Jan. 2011.

[37] S.-W. Hwang, H. Tao, D.-H. Kim, H. Cheng, J.-K. Song, E. Rill, M. a Brenckle, B. Panilaitis, S. M. Won, Y.-S. Kim, Y. M. Song, K. J. Yu, A. Ameen, R. Li, Y. Su, M. Yang, D. L. Kaplan, M. R. Zakin, M. J. Slepian, Y. Huang, F. G. Omenetto, and J.

A. Rogers, “A physically transient form of silicon electronics.,” *Science*, vol. 337, no. 6102, pp. 1640–1644, Sep. 2012.

[38] C. M. Boutry, H. Chandrahalim, P. Streit, M. Schinhammer, A. C. Hänzi, and C. Hierold, “Characterization of miniaturized RLC resonators made of biodegradable materials for wireless implant applications,” *Sensors Actuators, A Phys.*, vol. 189, pp. 344–355, 2013.

[39] E. Birdsell and M. G. Allen, “Wireless chemical sensors for high temperature environments,” *in Solid State Sensors, Actuators and Microsystems Workshop,* Hilton Head Island, USA, 2006, pp. 212–215.

[40] O. Akar, T. Akin, and K. Najafi, “A wireless batch sealed absolute capacitive pressure sensor,” *Sensors Actuators A Phys.*, vol. 95, no. 1, pp. 29–38, 2001.

[41] C. Zheng, W. Li, A.-L. Li, Z. Zhan, L.-Y. Wang, and D.-H. Sun, “Design and Manufacturing of a Passive Pressure Sensor Based on LC Resonance,” *Micromachines*, vol. 7, no. 5, p. 87, May 2016.

[42] M. Fonseca, M. G. Allen, J. Kroh, and J. White, “Flexible wireless passive pressure sensors for biomedical applications,” in *Solid State Sensors, Actuators and Microsystems Workshop,* Hilton Head Island, USA, 2006 , pp. 37–42.

[43] J. M. English and M. G. Allen, “Wireless micromachined ceramic pressure sensors,” in *IEEE Int. Conf. Micro Electro Mech. Syst.*, 1999., pp. 511–516

[44] M. Yvanoff, “LC Sensor for biological tissue characterization,” Doctoral dissertation, Rochester Institute of Technology, 2008.

[45] J. B. Ong, Z. You, J. Mills-Beale, E. L. Tan, B. D. Pereles, and K. G. Ong, “A Wireless, Passive Embedded Sensor for Real-Time Monitoring of Water Content in Civil Engineering Materials,” *IEEE Sens. J.*, vol. 8, no. 12, pp. 2053–2058, Dec. 2008.

[46] G. Stojanović, M. Radovanović, M. Malešev, and V. Radonjanin, “Monitoring of water content in building materials using a wireless passive sensor,” *Sensors*, vol. 10, no. 5, pp. 4270–4280, 2010.

[47] J. Voutilainen, “Methods and instrumentation for measuring moisture in building structures,” Doctoral dissertation, Helsinki University of Technology, 2005.

[48] T. J. Harpster, S. Hauvespre, M. R. Dokmeci, and K. Najafi, “A passive humidity monitoring system for in situ remote wireless testing of micropackages,” *J. Microelectromechanical Syst.*, vol. 11, no. 1, pp. 61–67, 2002.

[49] R. A. Potyrailo and C. Surman, “A passive radio-frequency identification (RFID) gas sensor with self-correction against fluctuations of ambient temperature,”

Sensors Actuators B Chem., vol. 185, pp. 587–593, Aug. 2013.

[50] R. A. Potyrailo, N. Nagraj, C. Surman, H. Boudries, H. Lai, J. M. Slocik, N. Kelley-Loughnane, and R. R. Naik, “Wireless sensors and sensor networks for homeland security applications.,” *Trends Analyt. Chem.*, vol. 40, pp. 133–145, Nov. 2012.

[51] R. A. Potyrailo, C. Surman, S. Go, Y. Lee, T. Sivavec, and W. G. Morris, “Development of radio-frequency identification sensors based on organic electronic sensing materials for selective detection of toxic vapors,” *J. Appl. Phys.*, vol. 106, no. 12, p. 124902, 2009.

[52] K. G. Ong, J. Wang, R. S. Singh, L. G. Bachas, and C. A. Grimes, “Monitoring of bacteria growth using a wireless, remote query resonant-circuit sensor: Application to environmental sensing,” *Biosens. Bioelectron.*, vol. 16, no. 4–5, pp. 305–312, Jun. 2001.

[53] M. S. Mannoor, H. Tao, J. D. Clayton, A. Sengupta, D. L. Kaplan, R. R. Naik, N. Verma, F. G. Omenetto, and M. C. McAlpine, “Graphene-based wireless bacteria detection on tooth enamel,” *Nat. Commun.*, vol. 3, p. 763, Mar. 2012.

[54] M. Bona, E. Sardini, M. Serpelloni, B. Andò, and C. O. Lombardo, “Study on a telemetrie system that works with an inkjet-printed resistive strain gauge,” in *IEEE Sensors Applications Symposium (SAS)*, 2016. pp. 1–6.

[55] W. Wu, “High Temperature Inductively Coupled Wireless Oxygen Sensor,” Doctoral dissertation, Carnegie Mellon University, 2011.

[56] J. Riistama, E. Aittokallio, J. Verho, and J. Lekkala, “Totally passive wireless biopotential measurement sensor by utilizing inductively coupled resonance circuits,” *Sensors Actuators A Phys.*, vol. 157, no. 2, pp. 313–321, Feb. 2010.

[57] B. E. Horton, S. Schweitzer, A. J. DeRouin, and K. G. Ong, “A Varactor-Based, Inductively Coupled Wireless pH Sensor,” *IEEE Sens. J.*, vol. 11, no. 4, pp. 1061–1066, Apr. 2011.

[58] R. Sarpeshkar, *Ultra Low Power Bioelectronics: Fundamentals, Biomedical Applications, and Bio-Inspired Systems*, 1st ed. Cambridge: Cambridge University Press, 2010.

[59] Y. Cheng and Y. Shu, “A New Analytical Calculation of the Mutual Inductance of the Coaxial Spiral Rectangular Coils,” *IEEE Trans. Magn.*, vol. 50, no. 4, 2014, Art. no. 7026806

[60] M. Soma, D. C. Galbraith, and R. L. White, “Radio-Frequency Coils in Implantable Devices: Misalignment Analysis and Design Procedure,” *IEEE Trans. Biomed. Eng.*, vol. BME-34, no. 4, pp. 276–282, Apr. 1987.

[61] S. Sauer, U. Marschner, B. Adolphi, B. Clasbrummel, and W.-J. Fischer, “Passive

Wireless Resonant Galfenol Sensor for Osteosynthesis Plate Bending Measurement," *IEEE Sens. J.*, vol. 12, no. 5, pp. 1226–1233, May 2012.

[62] M. H. Behfar, T. Björninen, E. Moradi, L. Sydänheimo, and L. Ukkonen, "Biotelemetric Wireless Intracranial Pressure Monitoring: An In Vitro Study," *Int. J. Antennas Propag.*, vol. 2015, 2015. Art. no. 918698.

[63] Agilent Technologies, "Agilent 4296B Netwok/Spectrum/Impedance Analyzer Option 010 Operating Handbook," Agilent Technologies, Japan, 2002. [Online]. Available: http://literature.cdn.keysight.com/litweb/pdf/04396-90046.pdf

[64] Agilent Technologies, "The Impedance Measurement Handbook: A Guide to Measurement Technology and Techniques," Agilent Technologies, USA, 2006. [Online]. Available: http://www.delftek.com/wp-content/uploads/2012/04/Agilent-Technologies-Impedance-Measurement-Handbook.pdf

[65] R. A. Potyrailo, "Multivariable Sensors for Ubiquitous Monitoring of Gases in the Era of Internet of Things and Industrial Internet," *Chem. Rev.*, vol. 116, no. 19, pp. 11877–11923, Oct. 2016.

[66] S. F. Pichorim and P. J. Abatti, "A novel method to read remotely resonant passive sensors in biotelemetric systems," *IEEE Sens. J.*, vol. 8, no. 1, pp. 6–11, 2008.

[67] R. Nopper, R. Niekrawietz, and L. Reindl, "Wireless Readout of Passive LC Sensors," *IEEE Trans. Instrum. Meas.*, vol. 59, no. 9, pp. 2450–2457, Sep. 2010.

[68] R. Nopper, R. Has, and L. Reindl, "A wireless sensor readout system-circuit concept, simulation, and accuracy," *IEEE Trans. Instrum. Meas.*, vol. 60, no. 8, pp. 2976–2983, 2011.

[69] E. Sardini and M. Serpelloni, "Wireless measurement electronics for passive temperature sensor," *IEEE Trans. Instrum. Meas.*, vol. 61, no. 9, pp. 2354–2361, 2012.

[70] R. A. Potyrailo, W. G. Morris, T. Sivavec, and H. W. Tomlinson, "RFID sensors based on ubiquitous passive 13.56-MHz RFID tags and complex impedance detection," *Wirel. Commun. Mob. Comput.*, vol. 9, no. 10, pp. 1318–1330, 2009.

[71] D. Marioli, E. Sardini, M. Serpelloni, and A. Taroni, "A new measurement method for capacitance transducers in a distance compensated telemetric sensor system," *Meas. Sci. Technol.*, vol. 16, no. 8, pp. 1593–1599, Aug. 2005.

[72] D. Marioli, E. Sardini, M. Serpelloni, and A. Taroni, "A distance compensated telemetric humidity sensor based on the parasitic capacitance variation," in *Proc. 2006 IEEE Instrumentation and Measurement Technology Conference*, Sorrento, Italy, 2006. pp. 655–660

[73] S. Sauer, U. Marschner, and W.-J. Fischer, "Detection coil independent frequency domain measurements for an inductively coupled resonant magnetoelastic

bending sensor," in *2011 IEEE SENSORS Proceedings*, 2011, pp. 2026–2029.

[74] E. Aittokallio, "Passiivinen resonanssianturi biopotentiaalien mittaukseen," Master's thesis, Tampere University of Technology, 2007.

[75] Analog Devices, "AD8302: LF-2.7 GHz RF/IF Gain and Phase Detector Data Sheet." Analog Devices, USA, 2002. [Online]. Available: http://www.analog.com/media/en/technical-documentation/data-sheets/AD8302.pdf

[76] T. Salpavaara, J. Verho, P. Kumpulainen, and J. Lekkala, "Wireless interrogation techniques for sensors utilizing inductively coupled resonance circuits," in *Procedia Engineering*, 2010, vol. 5, pp. 216–219.

[77] J. Lekkala, T. Salpavaara, J. Verho, and J. Riistama, "Simple inductively coupled resonance sensor for ECG and heart rate monitoring," in *Procedia Engineering*, 2010, vol. 5, pp. 1438–1441.

[78] A. Deluthault, V. Kerzerho, S. Bernard, F. Soulier, and P. Cauvet, "Efficient calibration of contact-less resonant bio-sensor affected by operating conditions," in *2016 IEEE 21st International Mixed-Signal Testing Workshop (IMSTW)*, 2016, pp. 1–6.

[79] M. Bona, E. Sardini, and M. Serpelloni, "Telemetric Model for Passive Resistive Sensors in Biomedical Applications," *Procedia Eng.*, vol. 87, pp. 444–447, 2014.

[80] P. Pasupathy, "Coupled Passive Resonant Circuits as Battery-free Wireless Sensors," Doctoral dissertation, The University of Texas at Austin, 2010.

[81] F. S. F. Ng ‐ Yip, "Medical Clothing: a tutorial paper on pressure garments," *Int. J. Cloth. Sci. Technol.*, vol. 5, no. 1, pp. 17–24, Jan. 1993.

[82] R. Duffield and M. Portus, "Comparison of three types of full-body compression garments on throwing and repeat-sprint performance in cricket players," Br. J. Sports Med., vol. 41, no. 7, pp. 409–414, Jan. 2007.

[83] J. S. Michael, S. N. Dogramaci, K. A. Steel, and K. S. Graham, "What is the effect of compression garments on a balance task in female athletes?," *Gait Posture*, vol. 39, no. 2, pp. 804–809, 2014.

[84] M. I. Trenell, K. B. Rooney, C. M. Sue, and H. Thompsson, Campbell, "Compression Garments and Recovery from Eccentric Exercise: A (31)P-MRS Study," *J. Sport. Sci. Med.*, vol. 5, pp. 106–114, 2006.

[85] A. M. Soto de la Cruz, "Pressure Sensors for Pressure Garment," Master's thesis, Tampere University of Technology, 2011.

[86] RAL German Institute for Quality Assurance and Labelling, "Medical Compression

Hosiery Quality Assurance RAL-GZ 287/1," Germany, 2008. [Online]. Available: http://www.tagungsmanagement.org/icc/images/stories/PDF/ral_gz_387_englisch.pdf

[87] E. Van den Kerckhove, S. Fieuws, P. Massagé, R. Hierner, W. Boeckx, J. P. Deleuze, J. Laperre, and M. Anthonissen, "Reproducibility of repeated measurements with the Kikuhime pressure sensor under pressure garments in burn scar treatment," *Burns*, vol. 33, no. 5, pp. 572–578, 2007.

[88] C. H. Y. Lai and C. W. P. Li-Tsang, "Validation of the Pliance X System in measuring interface pressure generated by pressure garment," *Burns*, vol. 35, no. 6, pp. 845–851, 2009.

[89] M. Ferguson-Pell, S. Hagisawa, and D. Bain, "Evaluation of a sensor for low interface pressure applications," *Med. Eng. Phys.*, vol. 22, no. 9, pp. 657–663, 2000.

[90] J. McLaren, R. J. N. Helmer, S. L. Horne, and I. Blanchonette, "Preliminary development of a wearable device for dynamic pressure measurement in garments," *Procedia Eng.*, vol. 2, no. 2, pp. 3041–3046, 2010.

[91] T. Salpavaara and P. Kumpulainen, "Modelling Nonlinear Responses of Resonance Sensors in Pressure Garment Application," *Artificial Intelligence Applications and Innovations. IFIP Advances in Information and Communication Technology,* vol 364, pp. 420–429, 2011

[92] J. R. Jang, "ANFIS: adaptive-network-based fuzzy inference system," *IEEE Trans. Syst. Man Cybern.*, vol. 23, no. 3, pp. 665–685, 1993.

[93] M. Järveläinen, "Towards In Situ Methods for Characterization of Porous Materials," Doctoral dissertation, Tampere University of Technology, 2016.

[94] B. Bitterlich, C. Lutz, and A. Roosen, "Rheological characterization of water-based slurries for the tape casting process," *Ceram. Int.*, vol. 28, no. 6, pp. 675–683, 2002.

[95] J. Tsubaki, M. Kato, M. Miyazawa, and T. Kuma, "The effects of the concentration of a polymer dispersant on apparent viscosity and sedimentation behavior of dense slurries," *Chem. Eng. Sci.*, vol. 56, no. 9, pp. 3021–3026, 2001.

[96] R. Wäsche, M. Naito, and V. A. Hackley, "Experimental study on zeta potential and streaming potential of advanced ceramic powders," *Powder Tecnol.*, vol. 123, no. 2-3, pp. 275–281, 2002.

[97] S. Lyu and D. Untereker, "Degradability of polymers for implantable biomedical devices," *Int. J. Mol. Sci.*, vol. 10, no. 9, pp. 4033–4065, 2009.

[98] S. Mukherjee and A. Gowen, "A review of recent trends in polymer

characterization using non-destructive vibrational spectroscopic modalities and chemical imaging," *Anal. Chim. Acta*, vol. 895, pp. 12–34, 2015.

[99] T. Salpavaara, J. Lekkala, S. Khan, V. Ellä, and M. Kellomäki, "Biodegradable encapsulation for inductively measured resonance circuit," in *2012 IEEE 12th International Conference on Bioinformatics and Bioengineering (BIBE)*, 2012, pp. 323–327.

[100] A. Antniemi, "Evaluation of the feasibility of biodegradable polymers for encapsulating resonance circuits," Master's thesis, Tampere University of Technology, 2016.

[101] S.-W. Hwang, X. Huang, J.-H. Seo, J.-K. Song, S. Kim, S. Hage-Ali, H.-J. Chung, H. Tao, F. G. Omenetto, Z. Ma, and J. A. Rogers, "Materials for bioresorbable radio frequency electronics.," *Adv. Mater.*, vol. 25, no. 26, pp. 3526–3531, Jul. 2013.

[102] T. Salpavaara, V. Ellä, M. Kellomäki, and J. Lekkala, "Biodegradable Passive Resonance Sensor - Fabrication and Initial Testing," in *Proc. International Conference on Biomedical Electronics and Devices*, 2015, pp. 127– 131.

[103] M. A. Brenckle, H. Cheng, S. Hwang, H. Tao, M. Paquette, D. L. Kaplan, J. A. Rogers, Y. Huang, and F. G. Omenetto, "Modulated degradation of transient electronic devices through multilayer silk fibroin pockets," *ACS Appl. Mater. Interfaces*, vol. 7, no. 36, pp. 19870–19875, 2015.

ORIGINAL PUBLICATIONS

P1

READOUT METHODS FOR AN INDUCTIVELY COUPLED RESONANCE SENSOR USED IN PRESSURE GARMENT APPLICATION

by

Salpavaara T., Verho J., Kumpulainen P. & Lekkala J., Dec. 2011

Sensors and Actuators A: Physical vol. 172, 109-116

https://doi.org/10.1016/j.sna.2011.02.051

P2

PERFORMANCE OF A NEAR-FIELD RADIO-FREQUENCY PRESSURE SENSING METHOD IN COMPRESSION GARMENT APPLICATION

by

Salpavaara T., Verho J. & Kumpulainen P., 2011

In Proceedings of Wireless Mobile Communication and Healthcare, MobiHealth 2011, Lecture Notes of the Institute for Computer Sciences, Social Informatics and Telecommunications Engineering vol. 83, 322-328

DOI: 10.1007/978-3-642-29734-2_44

P3

A MODEL BASED ANALYSIS OF THE MEASUREMENT ERRORS IN INDUCTIVELY COUPLED PASSIVE RESONANCE SENSORS

by

Salpavaara T. & Lekkala J., 2015

In Proceedings of XXI IMEKO World Congress, Prague, Czech Republic, Aug. 30 - Sep. 4, 2015

P4

PASSIVE RESONANCE SENSOR BASED METHOD FOR MONITORING PARTICLE SUSPENSIONS

by

Salpavaara T., Järveläinen M., Seppälä S., Yli-Hallila T., Verho J., Vilkko M., Lekkala J. & Levänen E., Nov. 2015

Sensors and Actuators B: Chemical vol. 219, 324-330

https://doi.org/10.1016/j.snb.2015.04.121

P5

INDUCTIVELY COUPLED PASSIVE RESONANCE SENSOR FOR MONITORING BIODEGRADABLE POLYMERS IN VITRO

by

Salpavaara T., Antniemi A, Hänninen A., Lekkala J. and Kellomäki M., Sep. 2016

Procedia Engineering vol. 168, 1304-1307

https://doi.org/10.1016/j.proeng.2016.11.353

UNPUBLISED MANUSCRIPT

M1

SIMULATION OF READOUT METHODS FOR INDUCTIVELY COUPLED PASSIVE RESONANCE SENSORS

by

Salpavaara T, Verho J. & Lekkala J.

Tampereen teknillinen yliopisto
PL 527
33101 Tampere

Tampere University of Technology
P.O.B. 527
FI-33101 Tampere, Finland

ISBN 978-952-15-4079-0
ISSN 1459-2045